



AMERICAN UNIVERSITY OF BEIRUT

INVESTIGATION ON CURCUMIN MEDIATED GREEN  
SOLID STATE SYNTHESIS OF CONJUGATED SILVER  
NANOPARTICLES AND ITS APPLICATION

by  
DINA SADEQ AL-NAMIL

A thesis  
submitted in partial fulfillment of the requirements  
for the degree of Master of Science  
to the Department of Chemistry  
of the Faculty of Arts and Sciences  
at the American University of Beirut


Beirut, Lebanon  
September 2017

AMERICAN UNIVERSITY OF BEIRUT

INVESTIGATION ON CURCUMIN MEDIATED GREEN  
SOLID STATE SYNTHESIS OF CONJUGATED SILVER  
NANOPARTICLES AND ITS APPLICATION

by  
DINA SADEQ AL-NAMIL

Approved by:

  
\_\_\_\_\_  
Dr. Digambara Patra, Associate Professor  
Chemistry, Department, AUB  
Advisor

  
\_\_\_\_\_  
Dr. Rabih Sultan, Professor  
Chemistry, Department, AUB  
Member of Committee

  
\_\_\_\_\_  
Dr. Faraj Hasanayn, Professor  
Chemistry, Department, AUB  
Member of Committee

Date of thesis defense: September 4, 2017

# AMERICAN UNIVERSITY OF BEIRUT

## THESIS, DISSERTATION, PROJECT RELEASE FORM

Student Name: AL-NAMIL

DINA

SADEQ

\_\_\_\_\_  
Last

\_\_\_\_\_  
First

\_\_\_\_\_  
Middle

Master's Thesis  
Dissertation

Master's Project

Doctoral

I authorize the American University of Beirut to: (a) reproduce hard or electronic copies of my thesis, dissertation, or project; (b) include such copies in the archives and digital repositories of the University; and (c) make freely available such copies to third parties for research or educational purposes.

I authorize the American University of Beirut, to: (a) reproduce hard or electronic copies of it; (b) include such copies in the archives and digital repositories of the University; and (c) make freely available such copies to third parties for research or educational purposes  
after : One ---- year from the date of submission of my thesis, dissertation, or project.

Two ---- years from the date of submission of my thesis, dissertation, or project.

Three ---- years from the date of submission of my thesis, dissertation, or project.

Dina Sadeq

September 18/2017

Signature

Date

## ACKNOWLEDGMENTS

Completing the Master has certainly been a long journey, and I would not have succeeded without the patience and the aid of my advisor Dr. Digambara Patra to whom I express my sincerest gratitude.

My sincere appreciation is also expressed to the committee members Dr. Rabih Sultan and Dr. Faraj Hassanyn for their valuable time, comments and suggestions.

I would like to thank my professors, Dr Kaafarani, Dr Halaoui, Dr Saliba and Dr Hmadeh, who made my learning experience throughout the past four years unique. I am also grateful to the personnel in the Central Research Science Laboratory for their technical support and assistance.

Special thanks to Elsy El Khoury for her help and support in the lab when I first arrived; and thanks to all the group members who worked or are still working with Dr. Patra's research group, Mazhar, Riham, Zeinab, Linda, Hassan....

Finally, I am thankful and blessed to have my family: my mom and dad for their unlimited support, my brother, my aunts, my uncles, my friend Darine for her support during the past three years, my favorite cousin Sarah because of her I came to Lebanon in the first place, all my cousins and my friends inside and outside Lebanon whose love and believe in me make me achieve my goals.

## AN ABSTRACT OF THE THESIS

Dina Sadeq AL-Namil for Master of Science  
Major: Chemistry

Title: Investigation on Curcumin Mediated Green Solid State Synthesis of Conjugated Silver Nanoparticles and its Application.

Metallic nanoparticles have considerably advanced in the field of nanotechnology for catalytic and sensor application; especially, silver nanoparticles (Ag NPs) have attracted extensive research interest due to their potential uses in catalytic and biomedical sensor development. Although preparation of Ag NPs could be simple and straight forward, the size distribution of synthesized Ag NPs and their application can be challenging. Achieving the mono-disperse nano-size and stable Ag NP products are still challenging. Of course, one emerging field to synthesize Ag NPs has been developing green synthetic routes due to (a) their environmental friendly methods to reduce waste, and (b) minimum possible toxicity of the materials formed. Curcumin is a member of ginger family and used as a spice, a cosmetics ingredient, a food flavoring and coloring reagent. Recently it is being used as supplement by various pharmaceutical companies and this market is exponentially growing. Curcumin is non-toxic and environmental friendly. In this thesis, I synthesized curcumin conjugated Ag NPs using a solid state green approach by using curcumin and  $\text{AgNO}_3$ . The synthetic condition optimized in four different temperatures  $4^\circ\text{C}$ , room temperature ( $\sim 20^\circ\text{C}$ ),  $40^\circ\text{C}$  and  $60^\circ\text{C}$  at ten different times, such as, 1, 2, 4, 8, 16 hours and 1, 2, 3, 5, and 7 days. This synthesis process gave us different size and shape of curcumin conjugated Ag NPs, which we investigated by various morphological and spectroscopic techniques. The growth of curcumin conjugated Ag NPs were studied in two different environments. In the first part, the growth medium was in an organic phase such as ethanol. Ag NPs obtained in this method were subsequently tested as catalysts for the reduction reaction of 4-nitrophenol to 4-aminophenol by using  $\text{NaBH}_4$  as a reducing reagent, as well as a bio-sensing agent for detecting different concentration of 6-O-palmitoyl-L-ascorbic acid. In the second part, growth medium during the solid state synthesized curcumin conjugated Ag NPs was in bio-surfactant solution such as rhamnolipids medium. In this medium we obtained smaller size particles, and these rhamnolipids stabilized Ag NPs were used as a biosensor for sensing different concentrations of L(-)Cystine, Bovine blood Serum Albumin (BSA) and Human blood Serum Albumin (HSA).

# CONTENTS

|                            |      |
|----------------------------|------|
| ACKNOWLEDGMENTS .....      | v    |
| ABSTRACT.....              | vi   |
| LIST OF ILLUSTRATIONS..... | viii |

## CHAPTER

|  |    |
|--|----|
| 1. INTRODUCTION .....  | 1  |
| 1.1. Green Chemistry .....   | 1  |
| 1.2. Nanomaterials .....   | 2  |
| 1.3. Solid state chemistry .....                                       | 3  |
| 1.4 Metallic Nano particles.....                                       | 4  |
| 1.4.1 Raman Effect .....   | 5  |
| 1.4.2 Localized Surface Plasmon Resonance (LSPR).....                  | 6  |
| 1.4.3 Synchronous Fluorescence vs. Resonance Rayleigh Scattering ..... | 6  |
| 1.5. Silver Nanoparticles (Ag NPs).....                                | 9  |
| 1.5.1 Silver (Ag) .....  | 9  |
| 1.5.2 Silver nanoparticles properties (Ag NPs) .....                   | 10 |
| 1.6. Application of silver nanoparticles .....                         | 11 |
| 1.7. Synthesis of Ag NPs .....   | 11 |
| 1.8. Curcumin .....  | 14 |
| 1.8.1 Origin and Source of Curcumin .....                              | 15 |

|  |           |
|--|-----------|
| 1.8.2 Isolation and extraction of Curcumin .....             | 16        |
| 1.8.3 Chemical structure of Curcumin/Curcumin molecule ..... | 18        |
| 1.9 Objective.....   | 19        |
| <br>   |           |
| <b>2. CURCUMIN CONJUGATED SILVER NPs GROWN IN</b>            |           |
| <b>ETHANOL MEDIUM .....</b>                                  | <b>20</b> |
| <br>   |           |
| 2.1. Introduction .....                                      | 20        |
| 2.1.1 Ascorbic acid .....                                    | 21        |
| 2.1.2 6-O-palmitoyl-L-ascorbic acid .....                    | 21        |
| 2.1.3 Oleic acid .....                                       | 22        |
| 2.1.4 Uric acid .....  | 22        |
| <br>   |           |
| 2.2. Materials .....   | 23        |
| 2.3. Instrumentation .....                                   | 23        |
| 2.4. Synthesis of curcumin conjugated Ag NPs .....           | 24        |
| 2.5. Result and dissection .....                             | 25        |
| 2.6. Characterization .....                                  | 26        |
| 2.7. Spectroscopic measurement .....                         | 33        |
| 2.8. Catalytic activity .....                                | 38        |
| 2.9. Testing sensing activity .....                          | 49        |
| <br>   |           |
| <b>3. CURCUMIN CONJUGATED SILVER NPs GROWN</b>               |           |
| <b>IN RHAMNOLIPIDS MEDIUM.....</b>                           | <b>53</b> |



|  |           |
|--|-----------|
| 3.1. Introduction .....  | 53        |
| 3.1.1 L(-)-Cystin .....  | 55        |
| 3.1.2 Bovine blood serum Albumin (BSA) .....                       | 56        |
| 3.1.3 Human blood serum Albumin (BSA) .....                        | 56        |
| 3.2. Materials .....   | 57        |
| 3.3. Instrumentation .....   | 57        |
| 3.4. Synthesis of curcumin conjugated Ag NPs .....                 | 58        |
| 3.5. Result and dissection .....                                   | 59        |
| 3.6. Characterizations .....                                       | 59        |
| 3.7. Spectroscopic measurement .....                               | 63        |
| 3.8. Sensing studies .....   | 66        |
| <b>4. CONCLUSION.....</b>  | <b>72</b> |
| <b>REFERENCE .....</b>   | <b>79</b> |
| <br><b>APPENDIX</b>  |           |
| 1. First order kinetics derivations .....                          | 76        |
| 2. Relation between particle size and surface to volume ratio..... | 77        |
| 3. Derivation for Estimating Binding Constant .....                | 78        |

# ILLUSTRATIONS

| Figure   | Page |
|--|------|
| 1.4. Jablonski diagram .....   | 9    |
| 1.8. Synthesis of curcumin by the general method proposed by Pabon.....  | 18   |
| 1.8. Keto-Enol tautomerism of curcumin.....  | 19   |
| 2.6. XRD pattern of curcumin conjugated Ag NPs prepared after 1day at 60°C.....  | 27   |
| 2.6. TGA of the curcumin conjugated Ag NPs sample prepared at 60°C and grown for 1 day.....  | 28   |
| 2.6. SEM images of curcumin conjugated Ag NPs in different growth time intervals at 4°C.....   | 30   |
| 2.6. SEM images of curcumin conjugated Ag NPs in different growth time intervals at 20°C.....  | 31   |
| 2.6. SEM images of curcumin conjugated Ag NPs in different growth time intervals at 40°C.....  | 32   |
| 2.6 SEM images of curcumin conjugated Ag NPs in different growth time intervals at 60°C.....   | 33   |
| 2.7. UV-VIS spectra of curcumin conjugated Ag NPs prepared at different growth time intervals for four different temperatures, (A) 60°C; (B) 40°C; (C) 20°C and (D) 4°C.....                 | 34   |
| 2.7. A) UV-VIS spectra of curcumin conjugated Ag NPs at the four different temperatures in one day growth sample. B) Absorbance ( $A_{max}$ ) vs temperatures for one day growth sample..... | 35   |
| 2.7. Fluorescence emission spectra of curcumin conjugated Ag NPs in different growth time intervals at 425 nm excitation wavelength, (A) 4°C; (B) 20°C; (C) 40°C and (D) 60°C.....           | 36   |
| 2.7. Fluorescence emission intensity at the maximum vs growth time in hours for curcumin conjugated Ag NPs at 425 nm excitation wavelength, (A) 4°C; (B) 20°C; (C) 40°C and (D) 60°C.....    | 37   |
| 2.7. Synchronous fluorescence spectra of curcumin conjugated Ag NPs in different growth time intervals at 425 nm excitation wavelength, (A) 4°C; (B)20°C; (C) 40°C and (D) 60°C.....         | 38   |

|  |    |
|--|----|
| 2.8. Change in the absorbance of 4-nitrophenol at ~400 nm in the presence of NaBH <sub>4</sub> without Ag NPs.....   | 40 |
| 2.8. Change in the absorbance of 4-nitrophenol at ~400 nm in the presence of NaBH <sub>4</sub> with curcumin conjugated Ag NPs prepared in different growth times at 20°C.....   | 41 |
| 2.8. Change in the absorbance of 4-nitrophenol at ~400 nm in the presence of NaBH <sub>4</sub> with curcumin conjugated Ag NPs prepared in different growth times at 40°C.....   | 42 |
| 2.8. Change in the absorbance of 4-nitrophenol at ~400 nm in the presence of NaBH <sub>4</sub> with curcumin conjugated Ag NPs prepared in different time at 60°C.....   | 44 |
| 2.8. Change in ln (A/A <sub>0</sub> ) with time during reduction of 4-nitrophenol in the presence of NaBH <sub>4</sub> with curcumin conjugated Ag NPs prepared at four different growth times at 60°C; (A) 7 days growth time, $\kappa = 0.035 \text{ s}^{-1}$ ; (B) 2 days growth time, $\kappa = 0.254 \text{ s}^{-1}$ ; (C) 1 day growth time, $\kappa = 0.341 \text{ s}^{-1}$ ; and (D) 1 hour growth time, $\kappa = 0.161 \text{ s}^{-1}$ ..... | 46 |
| 2.8. Change in ln (A/A <sub>0</sub> ) with time during reduction of 4-nitrophenol in the presence of NaBH <sub>4</sub> with curcumin conjugated Ag NPs prepared at two different growth times at 40°C; (A) 2 days growth time, $\kappa = 0.297 \text{ s}^{-1}$ and (B) 1 day growth time, $\kappa = 0.224 \text{ s}^{-1}$ .....  | 46 |
| 2.8. Change in ln (A/A <sub>0</sub> ) with time during reduction of 4-nitrophenol in the presence of NaBH <sub>4</sub> with curcumin conjugated Ag NPs prepared at 7 days growth time at 20°C, $\kappa = 0.294 \text{ s}^{-1}$ .....   | 47 |
| 2.8. Change in t <sub>1/2</sub> with the growth (preparation) times at four different temperatures, 20°C, 40°C and 60°C.....   | 48 |
| 2.8. The mechanism of Ag NPs as catalyst during reduction reaction for 4-NP.....   | 49 |
| 2.9. A) Fluorescence emission spectra of curcumin conjugated Ag NPs with different concentration of 6-O-palmitoyl-L-ascorbic acid, B) Alteration of fluorescence intensity of curcumin conjugated Ag NPs with different concentration of 6-O-palmitoyl-L-ascorbic acid.....  | 51 |
| 2.9. Fluorescence emission spectra of curcumin conjugated Ag NPs with different concentrations of Ascorbic Acid .....  | 51 |
| 2.9. Fluorescence emission spectra of curcumin conjugated Ag NPs with different concentrations of Uric Acid .....  | 52 |
| 2.9. Fluorescence emission spectra of curcumin conjugated Ag NPs with different concentration of Olic Acid .....   | 52 |
| 3.6. XRD pattern of curcumin conjugated and rhamnolipids stabilized Ag NPs prepared after 2 days of growth time at 60°C.....   | 60 |

|   |    |
|---|----|
| 3.6. SEM images of curcumin conjugated and rhamnolipids stabilized Ag NPs in different growth time intervals at 60°C.....   | 62 |
| 3.7. UV-VIS spectra of curcumin conjugated and rhamnolipids stabilized Ag NPs prepared in different growth time intervals at 60°C.....  | 63 |
| 3.7. (A) Fluorescence emission spectra of curcumin conjugated and rhamnolipids stabilized Ag NPs in different growth time intervals at 425 nm excitation wavelength, (B) Fluorescence intensity vs growth times in hours for curcumin conjugated and rhamnolipids stabilized Ag NPs in different growth time intervals.....   | 64 |
| 3.7. (A) Synchronous fluorescence spectra of curcumin conjugated and rhamnolipids stabilized Ag NPs in different growth time intervals at 425 nm excitation wavelength; (B) Synchronous fluorescence intensity vs (growth) times in hours for curcumin conjugated and rhamnolipids stabilized Ag NPs in different growth time intervals.....  | 65 |
| 3.8. (A) Fluorescence emission spectra of curcumin conjugated and rhamnolipids stabilized Ag NPs in the presence of various concentration of cystine; (B) Calibration curve for estimation of cystine by monitoring fluorescence intensity of curcumin conjugated Ag NPs; (C) Plot of cystine concentration vs. $(F - F_0)/F_0$ while determining association constant of cystine with curcumin conjugated and rhamnolipids stabilized Ag NPs ..... | 68 |
| 3.8. (A) Fluorescence emission spectra of curcumin conjugated and rhamnolipids stabilized Ag NPs in the presence of various concentration of BSA; (B) Calibration curve for estimation of BSA by monitoring fluorescence intensity of curcumin conjugated Ag NPs; (C) Plot of BSA concentration vs. $(F - F_0)/F_0$ while determining association constant of BSA with curcumin conjugated Ag NPs.....  | 69 |
| 3.8. (A) Fluorescence emission spectra of curcumin conjugated and rhamnolipid stabilized Ag NPs in the presence of various concentration of HSA; (B) Calibration curve for estimation of HSA by monitoring fluorescence intensity of curcumin conjugated Ag NPs; (C) Plot of HSA concentration vs. $(F - F_0)/F_0$ while determining association constant of HSA with curcumin conjugated Ag NPs.....   | 71 |

## TABLES

| Table   | Page |
|---|------|
| 1.7. Green synthesis of silver nanoparticles by different researchers using plant extracts..... | 13   |

# CHAPTER I

## INTRODUCTION

### 1.1 Green Chemistry

Green chemistry is an area of chemistry and chemical engineering for the design a product and process that can minimize the pollution and reduce consumption of nonrenewable resources. The first term of green chemistry related or associated with Paul Anastas of the US Environmental Protection Agency (EPA). In 1993 the EPA adopted the name (US Green Chemistry Program), and this was the central point for chemistry activities inside the United States which initiated the creation of the Presidential Green Chemistry Challenge Awards and the annual Green Chemistry and Engineering Conference. Before the 1990s there was a lot of research on green chemistry especially in Italy and United Kingdom, both had invented important procedures in green chemistry, recently in Japan Green and Sustainable Chemistry Network has been initiated. In 1999, the preliminary edition of Green Chemistry journal appeared, and it was sponsored by the Royal Society of Chemistry. Paul Anastas has designed 12 principles in green chemistry, and those 12 principles can be paraphrased as <sup>1</sup>:

1. Waste should be prevented better than be remedied.
2. The design should have nontoxic or nonhazardous product.
3. The efficiency should be in atomic level.
4. The design should give safer products.
5. The procedure should use innocuous solvents and auxiliaries.
6. The design should be energy efficient.

7. The procedure preferably should use renewable raw materials.
8. The synthesis procedure should be shorter, such as, it should avoid derivatization.
9. The reagent should be catalytic rather than stoichiometric.
10. It should design products for degradation.
11. It should develop analytical methodologies for pollution prevention.
12. The processes should be inherent.

## **1.2 Nanomaterials**

In the past few decades, nanomaterials or nanoparticles have shown their ability to contribute in many applications because of their small size and large surface area to volume ratio, and this what give them distinct chemical and physical properties like mechanical properties, biological and satirical properties, catalytic activity, thermal and electrical conductivity, optical absorption and melting point. Whereas the size of nanoparticles range from 1-100 nm, all of these properties are different with their bigger counterparts. Therefore, nanomaterials or nanoparticles have size and shape-dependent properties; it means that different size and shapes can give different properties as well as different applications ranging from bio-sensing and catalysts to optics, antimicrobial activity, computer transistors, electrometers, chemical sensors, and wireless electronic logic and memory schemes. So one can synthesize nanoparticles of different shapes and sizes by controlling the synthetic process <sup>2</sup>.

### 1.3 Solid State Synthesis

Solid state materials have the most structural diversity, solids in chemistry contain molecules, atoms and ions that are statically positioned. If we want to understand and have a full knowledge about the solids materials, we need to know the structural interactions between the subunit atoms, ions, and molecules. Solid materials can be classified into amorphous and crystalline materials. If the atoms, ions or molecules arranged themselves into a lattice or regular arrangements with regularly repeating units formed on a long range, then it is called crystalline materials, as exemplified by crystalline minerals in nature which take many years to form under extreme temperature and pressure, or slow evaporation processes. The amorphous materials are made when no long-range structural order throughout the solid. The solid product can be synthesized from many chemical reactions, and it will form an amorphous material by default, but if special procedures are used to facilitate molecular arrangement, then a crystal will form. The crystalline state of material is thermodynamically favored, but the formation of amorphous materials is kinetically favored. The properties of amorphous and crystalline solids in general depend on the intermolecular and intramolecular interactions between its subunits, and each amorphous and crystalline solid material contains certain types of those intermolecular and intramolecular interactions. The physical, optical, and electronic properties of amorphous and crystalline solid depend on the strength of the interactions between the subunits. For example, the intramolecular forces such as (atomic separation, inter-atomic bonding energies) directly influence the conductivity, thermal expansion, and elasticity of a material. However intermolecular forces influence the melting, boiling and sublimation point, solubility, and vapor pressure of a material <sup>3</sup>.



Normally organic and inorganic materials are often prepared in a solvent environment, however, in solid state synthesis, materials are prepared in solid state by mixing/grinding. Solid state synthetic approach limits the use of solvent and can create unique morphologies and compositions necessary to generate the desired attributes in scintillation crystals, piezoelectrics, and other advanced materials. Use of solid state synthetic procedure can be a green approach to prepare materials of desired functionalities. Combination of such methods during preparation of nanoparticles to control matter at the molecular level will have greater advantages for various applications. Thus, when we combine nanotechnology application and the principles and practices of green chemistry by using the term “green nanotechnologies”. This new technology has become a key component of the nanotechnology future, and also may hold the key to an environmentally sustainable society in the twenty-first century <sup>4</sup>.

#### **1.4 Metallic Nanoparticles**

Metallic nanoparticles have fascinated the scientist for over a century in both research and technology because of the presence of Plasmon resonance in the nano-sized particles, when the light interacts with matter <sup>3</sup>. This property is not available in isolated molecules or bulk metals; therefore, they are important in many applications in catalysis, sensing and imaging. This interaction happens because the nanoparticles conducting electrons have a large density and their size is confined to dimensions smaller than the mean free path. The size and shape of the particle as well as the dielectric function of the surrounding medium determine the frequency and the strength of the resonance <sup>6</sup>. Nowadays metallic nanoparticles can be modified and synthesized by attaching them to

various chemical functional groups like attaching them to antibodies, ligands or drugs of interest which allows them to be useful in a wide range of potential applications in biotechnology, magnetic separation, pre-concentration of target analytes, targeted drug delivery, vehicles for gene and drug delivery and more importantly diagnostic imaging <sup>5</sup>. The metallic nanoparticles have optical properties, such as Raman Effect, that are used in many of today's applications involving nanoparticles.

#### ***1.4.1 Raman Effect***

In Raman Effect the incident light is elastically scattered from a sample or molecules and thus, the frequency of the incident light is shifted to a higher vibrational level. Since this effect was discovered in 1927, it has drawn a lot of attention from the basic research point of view as a powerful spectroscopic technique with many practical applications. The invention of laser light sources with monochromatic photons of high flux densities was a climax of Raman spectroscopy in history, and this resulted in a very important improvement in scattering signals. The lasers development opened the field of stimulated or coherent Raman spectroscopies, in which molecular vibrations are coherently excited. The intensity of spontaneous Raman scattering depends linearly on the number of probed molecules, where the coherent Raman signal is proportional to the square of the probed molecules number, therefore, coherent Raman techniques can provide interesting new opportunities such as vibrational imaging of biological samples <sup>6</sup>. The ability of metal nanoparticles to enhance the Raman scattering fold is a proven fact that qualified a very sensitive detection analytics for single molecule levels. This ability was first published in 1977 <sup>6</sup>.

### ***1.4.2 Localized Surface Plasmon Resonance (LSPR)***

LSPR frequency depends on the nanoparticles and on the medium that it can disband in it. There are two important results can be shown from this dependency, firstly, the LSPR is tunable which means its frequency can be changed through the changes in the nanoparticle size and shape. Secondly, metal nanoparticles are sensitive to their local environment, for example, if the dielectric properties of their medium changed the LSPR will shift and it can be measured. The tunability and sensitivity of LSPR can be used for the metal nanoparticles in the materials of choice for optical sensing and imaging applications <sup>4</sup>.

Metallic nanoparticles are mostly prepared from noble metals like silver (Ag), gold (Au), palladium (Pd), and platinum (Pt), those metals display a Plasmon resonances in the visible spectrum regime, but silver (Ag) exhibits the highest efficiency of Plasmon excitation <sup>7</sup>.

### ***1.4.3 Synchronous Fluorescence vs. Resonance Rayleigh Scattering***

Luminescence is the emission of light from any substance and happens due to the relaxation from electronically excited state. Luminescence is classified into fluorescence and phosphorescence depending on the nature of the excited state. In singlet excited state the electron in the orbital is paired (opposite spin) to the second electron in the ground state orbital. The return of electron to the ground state is possible when the spin is allowed and occurs rapidly by emission of a photon. The absorption and emission of light are illustrated by Jablonski diagram. Jablonski diagrams are used in different

forms, and they can illustrate various molecular processes that can occur in excited states. This diagram is named after Professor Alexander Jablonski (Figure 1), who is regarded as the father of fluorescence spectroscopy. Fluorescence spectroscopy is considered to be simple, non-destructive, non-invasive and relatively inexpensive analytical method <sup>8</sup>. In fluorescence measurement, we can measure an emission spectrum for a sample by making a scan for the emission monochromator at various emission wavelengths,  $\lambda_{em}$ , at a particular excitation wavelength  $\lambda_{ex}$ . In excitation spectrum, on the other hand the excitation monochromator is scanned at various excitation wavelengths  $\lambda_{ex}$  by keeping the emission monochromator constant at a particular wavelength. But if we want to analyze multi-component system, in some cases using the single wavelength fluorescence measurement, the analysis will not be efficient due to the overlapping between the emission and excitation spectra. This problem can be solved by using a synchronous fluorescence spectroscopy (SFS) where the overlapping spectra can be minimized. Therefore, the synchronous fluorescence spectrum can be described as a spectrum where we can scan both the emission and excitation monochromators simultaneously. The SFS technique depends on the scan rate, so when we have a constant scan rate for both of the monochromators then we will have a constant wavelength interval  $\Delta\lambda$  between  $\lambda_{ex}$  and  $\lambda_{em}$ , this technique is known as constant-wavelength SFS. The synchronous fluorescence spectra have sharp and narrow peaks as explained by Jablonski diagram, depicted in figure 1 <sup>34</sup>, where a molecule excited from a different level in the ground state starting from wavelength  $A_1, A_2, \dots, A_9$  and could give fluorescence in the wavelength  $F_1, F_2, \dots, F_9$ . The fluorescence emission spectrum of a fluorophore remains unchanged, without taking into account excitation wavelength, but we will notice a variation in the

fluorescence intensity because it depends on the probability of the electronic transition of the molecule.

The fluorescence emission spectrum happens when the molecules are excited at the highest absorption level  $A_5$  then the fluorescence is collected in all the emission wavelengths vibrational levels  $F_1, F_2, F_3, \dots, F_9$ . While the fluorescence excitation spectrum obtained by exciting the molecules at all different excitation wavelength vibrational levels  $A_1, A_2, \dots, A_9$ , and the fluorescence is collected only at the highest emission level  $F_5$ . But in the synchronous fluorescence spectra SFS, a specific interval wavelength is chosen so a signal is observed only when  $\Delta\lambda$  matches the interval between one absorption band and one emission band. For example, at  $\Delta\lambda = A_5 \sim F_5$  case we will not see any fluorescence signal until the excitation monochromator is at  $A_5$  and fluorescence wavelength is at  $F_5$ , then respectively the molecules are excited at  $A_6, A_7, \dots, A_9$  and corresponding fluorescence are recorded at  $F_6, F_7, \dots, F_9$ .  $\Delta\lambda$  defines “the matching of absorption and emission band”. The process continues to happen until a full spectrum is recorded<sup>9</sup>. Therefore, by keeping the  $\Delta\lambda = 0$ , resonance Rayleigh scattering of nanoparticles can be measured.

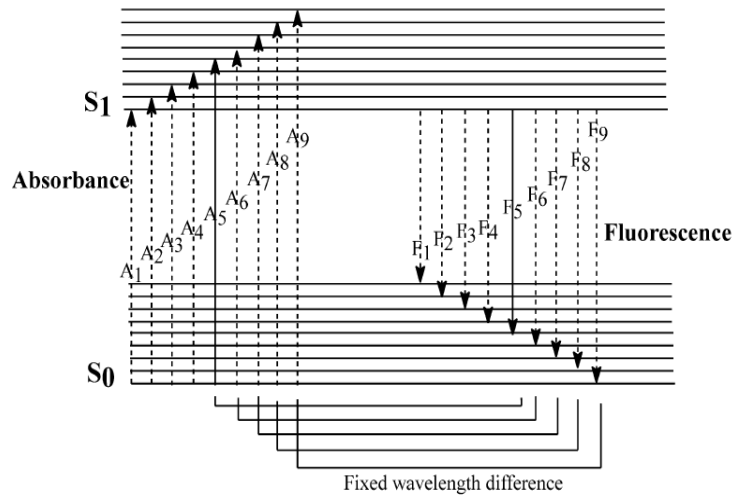


**Figure 1: Jablonski diagram**

## 1.5 Silver Nanoparticles (Ag NPs)

### 1.5.1 Silver (Ag)

Silver a soft, white transition metal, occurs either naturally in its free form as a pure element, or as an alloy with gold and other metals. It also can be found in minerals like argentite and chlorargyrite. Ag has the highest electrical conductivity of all elements and the highest thermal conductivity of all metals. Most silver is obtained as a by-product of copper, gold, lead, and zing refining <sup>10</sup>. Silver is a more affordable metal than gold, palladium and platinum. Silver is the only material whose Plasmon resonance can be tuned to any wavelength in the visible spectrum <sup>6</sup>.

### ***1.5.2 Silver nanoparticles properties (Ag NPs)***

Silver nanoparticles (Ag NPs) have shown optical properties better than other noble metallic nanoparticles due to the discovery of a surface enhanced Raman scattering, which is due to the locally increased electromagnetic field a consequence of Plasmon resonance <sup>4</sup>. The single Ag NP can interact efficiently more than any other particles with the same dimension to any known organic or inorganic chromophores, Ag NPs and their assemblies are responsible for the enhancement of fluorescence, absorption, photochemical, and nonlinear phenomena <sup>4</sup>. The Ag NPs capture more light than the light physically incident on them, because of the light interaction cross-section for silver can be about ten times that of the geometric cross-section <sup>6</sup>.

On the other hand, Ag NPs show antimicrobial properties, where Ag NPs act as effective killing agents against Gram negative bacteria and Gram positive bacteria.

- Gram negative bacteria include Acinetobacter, Escherichia, Pseudomonas, Salmonella, and Vibrio. Some of these bacteria needed a special treatment like Acinetobacter species which are associated with nosocomial infections that need a treatment in a hospital or a healthcare service unit.
- Gram positive bacteria include Bacillus, Clostridium, Enterococcus, Listeria, Staphylococcus, and Streptococcus.
- Antibiotic resistant bacteria include strains such as methicillin resistant and vancomycin resistant Staphylococcus aureus, and Enterococcus faecium. Silver nanoparticles (Diameter 5-32 nm) enhance the antibacterial activity of various antibiotics. The antibacterial activities of penicillin G, amoxicillin, erythromycin,

clindamycin, and vancomycin against *Staphylococcus aureus* and *Escherichia coli* increase in the presence of silver nanoparticles.

Ag NPs have also antifungal properties, where they act as fungicides against common fungi like *Aspergillus*, *Candida*, and *Saccharomyces*. The exact mechanism of how Ag NPs functions against fungi is not clear yet, therefore, the mechanism of antibacterial actions has not been proposed for fungi. Silver nanoparticles (diameter  $13.5 \pm 2.6$  nm) are effective against yeast isolated from bovine mastitis <sup>11</sup>.

## **1.6 Application of silver nanoparticles**

Ag NPs have wide applications in many areas such as integrated circuits <sup>12</sup>, sensors, biolabelling, filters <sup>13</sup>, antimicrobial deodorant fibers <sup>14</sup>, cell electrodes <sup>15</sup>, and antimicrobials <sup>16,17</sup>. Because of antimicrobial properties of Ag NPs, we can use them in different fields of medicine, various industries, animal husbandry, packaging, accessories, cosmetics, health and military <sup>18,19</sup>. Ag NPs applications in medical can be divided into two types: diagnostic and therapeutic uses <sup>20</sup>.

## **1.7 Synthesis of Ag NPs**

A variety of techniques have been developed to synthesize Ag NPs, which include laser irradiation technique <sup>21</sup>, photochemical reduction <sup>22</sup>, electrochemical or sonochemical deposition <sup>23,24</sup>, aerosol technique <sup>25</sup> etc. Each method has advantages and disadvantages with common problems being costs, scalability, particle sizes and size distribution <sup>26</sup>. Another method of preparation is by using a reducing agent such as sodium citrate,








ascorbate, sodium borohydride ( $\text{NaBH}_4$ ), elemental hydrogen, polyol process, Tollens reagent, N,N-dimethylformamide (DMF), and poly (ethylene glycol)-block copolymers, which are used for reduction of silver ions ( $\text{Ag}^+$ ) in aqueous or non-aqueous solutions. These reducing agents reduce  $\text{Ag}^+$  and lead to the formation of metallic silver ( $\text{Ag}^0$ ), which is followed by agglomeration into oligomeric clusters. These clusters eventually lead to the formation of metallic colloidal silver particles<sup>27,28</sup>.



In some cases, the synthetic and applications of silver nanoparticles can be linked together or depend on each other, for example in pharmacological applications like in antimicrobial activity, the *Boerhaavia diffusa* that were used in synthesis of Ag NPs showed higher sensitivity against *Flavobacterium branchiophilum* than the other two fish bacterial pathogens *Aeromonas hydrophila* and *Pseudomonas fluorescens*. Lingonberry and cranberry juice assisted Ag NPs are found to be more active against *S. aureus*, *B. subtilis*, and *B. cereus* and less active against *C. albicans* and food borne *B. Silver nanoparticles synthesized using *Acalypha indica* Linn show only 40% cell inhibition against human breast cancer cells (MDA-MB-231). While *Datura innoxia* Ag NPs inhibited 50% proliferation of human breast cancer cell line MCF7 at 20  $\mu\text{g}/\text{mL}$  after 24 hours incubation by suppressing its growth, arresting the cell cycle phases, and reducing DNA synthesis to induce apoptosis.*

In miscellaneous applications like water treatment stable Ag NPs synthesized using *Anacardium occidentale* fresh leaf extract at 80°C has been used as a novel probe for sensing chromium ions [Cr (VI)] in tap water. In catalytic activity, *Acacia Nilotica* pod mediated Ag NPs modified glassy carbon electrode has been reported to have greater catalytic activity on the reduction of benzyl chloride compared to those of glassy carbon

and metallic Ag electrode. The synthesized Ag NPs using *Gloriosa superba* extract has been found to act through the electron relay effect and influence the degradation of methylene blue at the end of the 30 min <sup>29</sup>. Some of the green synthetic procedures using plant extracts to prepare Ag NPs and their size and shapes are summarized in Table 1.

**TABLE 1:** Green synthesis of silver nanoparticles by different researchers using plant extracts

| Plant   | Size in nm | Shapes                      | References |
|---|------------|-----------------------------|------------|
| <i>Acalypha indica</i>           | 0.5-30nm   | Spherical                   | 26         |
| <i>Datura inoxia</i>            | 16-40nm    | Quasilinear superstructures | 26         |
| <i>Boerhaavia diffusa</i>      | 25nm       | Spherical                   | 26         |
| <i>Gloriosa superba</i>        | 3-20nm     | Spherical                   | 30         |
| <i>Anacardium occidentale</i>  | 36-56nm    | Spherical                   | 31         |

|   |                |                         |           |
|---|----------------|-------------------------|-----------|
| <p><b>Lingonberry</b></p>      | <p>6-60nm</p>  | <p>Different shapes</p> | <p>20</p> |
| <p><b>Acacia Nilotica</b></p>  | <p>10-40nm</p> | <p>Spherical</p>        | <p>32</p> |

### 1.8 Curcumin

Curcumin is a bright yellow chemical material derived from rhizome of turmeric.

Although curcumin was known to scientists, for at least two centuries, it continues to attract researchers from all over the world. Curcumin was first isolated from turmeric in around 1815, however until the 1970s there were only few reports published on its chemical structure, synthesis, biochemical and antioxidant activity. Following Aggarwal and co-workers in 1990s on its potential anticancer activity, there was rapid growth of curcumin research with more than 14,000 citations on curcumin to date. The majority of researchers were interested in the biological aspects of curcumin, and only few tried to understand the importance of the chemistry of curcumin responsible for its distinctive biological activity. Curcumin research has become one of the most favorite subjects for the main branches of chemistry, including organic, inorganic, physical and analytical chemists. The main focus of research in organic chemistry was the extraction and synthesis of curcumin and new synthetic derivatives. The inorganic chemists used the

ability of curcumin in chelating metals through the  $\beta$ -diketo group to form novel structural entities that have modified biochemical activities. The physical chemists were more interested in the highly sensitive spectroscopic properties of curcumin and studied its interactions with microheterogeneous systems and biomolecules. The main focus of analytical chemists was on curcumin's unique absorption spectroscopic properties to identify and quantitatively estimate trace elements like for example estimation of boron, as a red colored product. The biological activity of curcumin that was investigated by other chemistry studies were useful in understanding its chemical reactivity with reactive oxygen species (ROS), addition reactions, degradation and formation of nano conjugates and formulations.

### ***1.8.1 Origin and Source of Curcumin***

Turmeric which is *Curcuma longa* L, the source of curcumin, is cultivated in tropical and subtropical regions. India is considered as the largest producer of turmeric worldwide, where it has been used as a home-remedy for several ailments for several decades. Turmeric contains varied amounts of curcuminoids ranging between 2%–9%. The variation is related to the origin and the soil conditions where curcumin was grown. Curcuminoid include a group of compounds such as curcumin, demethoxycurcumin, bis-demethoxycurcumin and cyclic curcumin. Curcumin is considered as the major component of curcuminoid.

### ***1.8.2 Isolation and extraction of Curcumin***

The extraction and separation of curcumin from turmeric powder was described more than 200 years ago, however, researchers continued to identify more improved and advanced extraction methods until the present time.

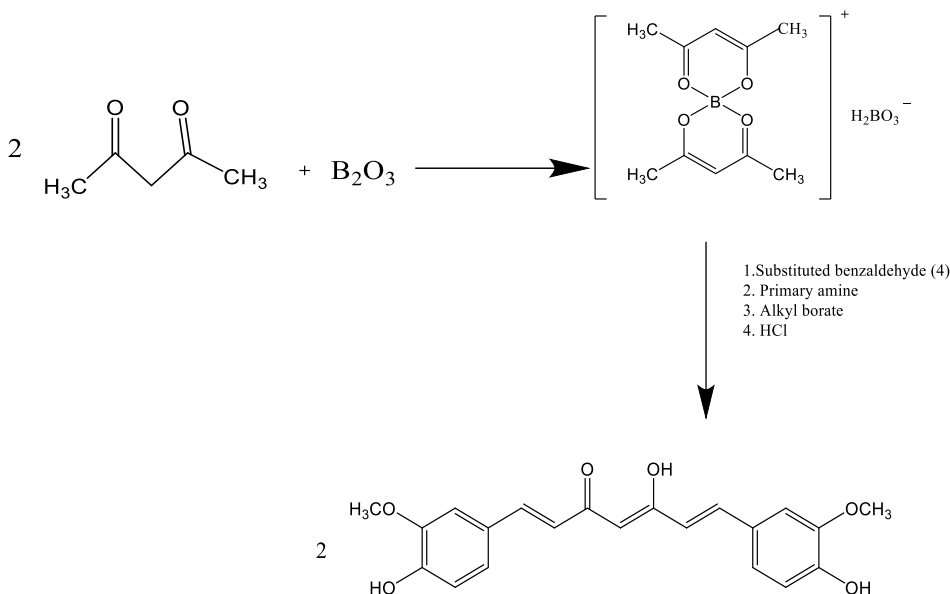
Solvent extraction followed by column chromatography is considered the most commonly used method for separating curcumin from turmeric. In this method, various polar and non-polar organic solvents have been used such as, ethylacetate, hexane, methanol and acetone. However, ethanol is widely used and deemed to be the preferred solvent for extracting curcumin.

Column chromatography can be used to separate curcumin from mixtures containing curcumin mixed with demethoxycurcumin and bisdemethoxycurcumin. In column chromatography, the mixture is adsorbed on silica gel using mixtures of solvents such as dichloromethane/acetic acid or methanol/chloroform to yield the three components in three different fractions. The curcumin fraction can be further purified on silica gel and then eluted using chloroform/dichloromethane and ethanol/methanol mixtures.

High performance liquid chromatography (HPLC) has been employed for the detection and estimation of curcumin. The reverse phase C18 columns is used as stationary phase and different gradients of solvents containing acetonitrile/water or chloroform/methanol as the mobile phase. For detection of curcumin in the absorption detectors the wavelength range from 350 to 450 nm, or in the UV region by using a common detection wavelength in the range of 250 to 270 nm. Liquid chromatography-coupled mass spectrometry is considered as another good tool for detecting curcumin. However, the fluorescence method is considered as the most sensitive methods for detection of curcumin, it can

detect up to 1 ng/mL, by exciting in the 400 to 450 nm region. High-performance-thin layer chromatography methods using aluminium plates precoated with silica gel as stationary phase and chloroform-methanol as solvent are considered very useful for both detection and separation of curcumin. The micro emulsion electro kinetic chromatography using oil droplets and surfactants has been shown to be useful for the extraction as well as the estimation of curcumin in food and medicinal samples. Capillary electrophoresis with amperometric detection can be routinely employed to estimate curcumin/turmeric in food materials. HPLC and LC/MS have been demonstrated to have the ability to detect minute quantities of curcumin in biofluids to evaluate the pharmacokinetics, biodistribution and metabolism<sup>33</sup>. Pabon has reported a simple method for the synthesis of curcumin in high yields using acetyl acetone and substituted aromatic aldehydes in the presence of boron trioxide ( $B_2O_3$ ), trialkyl borate and *n*-butylamine. This method has been adopted by several other research groups for practical synthesis of curcumin<sup>34</sup>. The primary step is the reaction of 2,4-diketones with suitably substituted aromatic aldehydes, and to prevent participation of the diketone in Knoevenagel condensations it is complexed with boron. The curcumin can be separated easily from the reaction by using anhydrous conditions and polar aprotic solvents. Here, primary and secondary amines are used as catalysts to provide the necessary basicity to deprotonate the alkyl groups of the diketone. Water was produced in the reaction during the condensation scavengers like alkyl borates, and the water can react with the diketone complex, thereby reducing the curcumin yield. The boron complex dissociates into curcumin under slightly acidic conditions. Curcumin from this reaction mixture can be

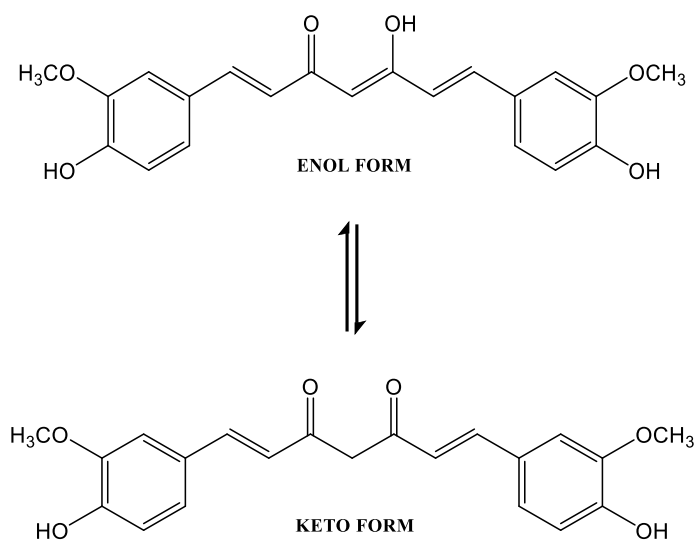
separated by washing and repeated precipitation followed by column chromatography, as in the scheme below:



**Scheme 1: Synthesis of curcumin by the general method proposed by Pabon**

### 1.8.3 Chemical structure of Curcumin molecule

Curcumin is a symmetric molecule, also known as diferuloyl methane. The IUPAC name of curcumin is (1*E*,6*E*)-1,7-bis(4-hydroxy-3-methoxyphenyl)-1,6-heptadiene-3,5-dione, with chemical formula  $\text{C}_{21}\text{H}_{20}\text{O}_6$ , and molecular weight of 368.38. It has three chemical entities in its structure: two aromatic ring systems containing *o*-methoxy phenolic groups, connected by a seven carbon linker consisting of an  $\alpha,\beta$ -unsaturated  $\beta$ -diketone moiety. The chemical structure of curcumin is given in Scheme 2. The diketo group exhibits keto-enol tautomerism, which can exist in different types of conformers depending on the environment <sup>33</sup>.



**Scheme 2: Keto-Enol tautomerism of curcumin**

## 1.9 Objectives

In this thesis work I attempt for the synthesis of Ag NPs using curcumin via solid state green synthetic approach, this is a first attempt in literature to prepare curcumin conjugated Ag NPs using a solid state synthetic procedure. Curcumin was used because it is not toxic and safe, thus, it can be a very good candidate to prepare nanoparticles through green synthetic route. Synergetic reducing approach has been developed by our laboratory for the synthesis of silver nano-particles using the curcumin as reducing agent at room temperature (around 20°C), 4°C, 40°C and 60°C respectively. The temperature can have an effect on the size and the shape of silver nanoparticles. The role of temperature in the formation and growth of silver nanoparticles will be identified by scanning electron microscopy (SEM) and UV–VIS spectrometer techniques. Finally, the prepared curcumin conjugated Ag NPs will be tested as catalyst for the reduction reaction of p-nitrophenol, and for optical sensing applications like biomedical applications.



## CHAPTER II

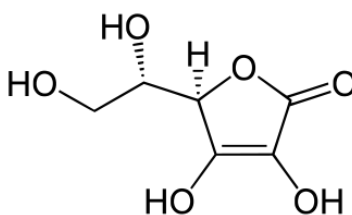
# CURCUMIN CONJUGATED SILVER NPs GROWN IN ETHANOL MEDIUM

### 2.1. Introduction

Synthesis of silver nanoparticles is an area that has witnessed a lot of interest during the past decades<sup>35</sup>. Nanoparticles have unique electrical, optical, magnetic, and chemical properties different than their bulk match. The properties of Ag NPs are determined by parameters such as size, shape, composition or crystalline structure. Those unique properties make the Ag NPs used in wide range of potential applications in different fields such as medicine, biotechnology and catalysis, also placing colloidal nanoparticles among the most intensely studied nanoscale materials. However, it is possible to control Ag NPs properties in the desired manner by changing one of the above listed parameters, tailored to a specific use, which is an important way to understand the requirements for formation processes<sup>36</sup>. The main applications of silver nanoparticles are found in catalysis and as bactericides<sup>1</sup>. In my research, I prepared Ag NPs using a solid state procedure and tested their catalytic activities for the reduction of 4-nitrophenol to 4-aminophenol by using NaBH<sub>4</sub> as a reducing agent. Furthermore these materials were also tested as optical sensor for 6-O-palmitoyl-L-ascorbic acid, Ascorbic acid, Oleic acid and Uric acid each one of those materials has specific properties and different structures.

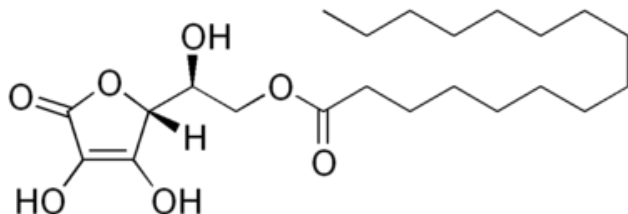
### 2.1.1 Ascorbic acid

Ascorbic acid, also known as Vitamin C, is a water soluble micronutrient used or involved in many multiple biological functions and it is a strong reducing agent. Ascorbic acid is acid contain an enediol group built into a five membered heterocyclic lactone ring. The chemical and physical properties of ascorbic acid are related to its structure <sup>37</sup>, which is given below:



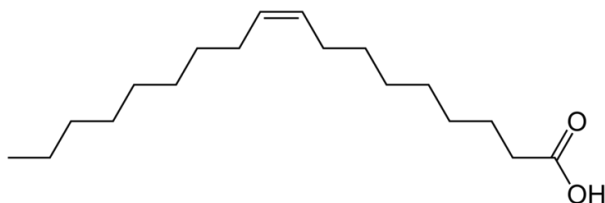
### 2.1.2 6-O-palmitoyl-L-ascorbic acid

It is a fat soluble form of vitamin C (vitamin C ester) formed from ascorbic acid and palmitic acid. It is used as a source of vitamin C, antioxidant and food additive approved by EU and other countries. 6-O-palmitoyl-L-ascorbic acid can break down through digestive process into ascorbic acid and palmitic acid before being absorbed by bloodstream <sup>38</sup>, the structure is shown below:



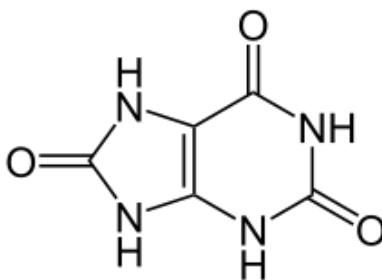
### 2.1.3 Oleic acid

Oleic acid is a fatty acid classified as a monounsaturated omega-9 fatty acid, and it occurs naturally in many animals and vegetables oils. The term "oleic" means related to, or derived from, and mostly refers to olive oil. The main use of oleic acid occurs as a component in many foods in the form of triglyceride, and it is soluble in ethanol, the structure is given below <sup>39</sup>:



### 2.1.4 Uric acid

Uric acid is a heterocyclic compound, and is a product of the metabolic breakdown of purine nucleotides. High blood concentration of uric acid can cause gout, diabetes and the formation of ammonium acid urate kidney stones. Also it is a normal component of urine, the structure is given below <sup>40</sup>:



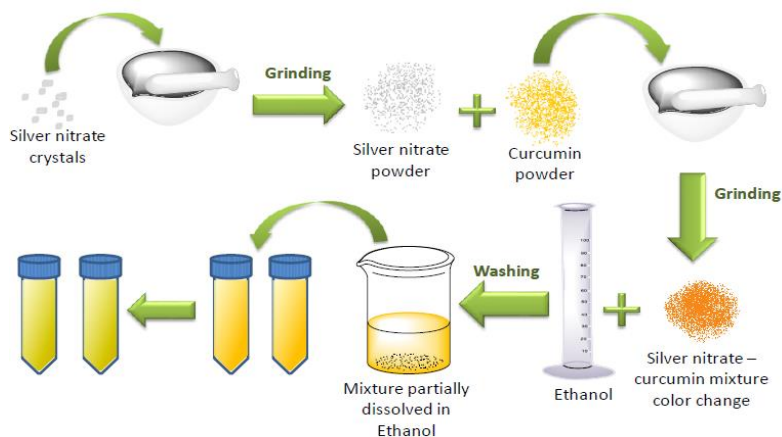
## 2.2. Materials

Curcumin, silver nitrate, p-nitro phenol and ethanol were all obtained from Sigma–Aldrich and directly used without further purification. For sensing experiment 12.4 mg of 6-O-palmitoyl-L-ascorbic acid in 3 mL ethanol, 5.3 mg of ascorbic acid in 3 mL double distilled water (DDW), 8.5 mg of oleic acid in 3 mL ethanol and 5.04 mg of uric acid in 3 mL DDW were used for preparing stock solutions. For catalysis 3.4 mg of sodium borohydride ( $\text{NaBH}_4$ ) in 3 mL DDW was prepared freshly.

## 2.3. Instrumentation

The absorption spectra were recorded at room temperature using a JASCO V-570 UV–VIS–NIR spectrophotometer. X-Ray diffraction (XRD) data were collected using a Bruker d8 discover X-Ray diffractometer equipped with Cu-K $\alpha$  radiation ( $\lambda = 1.5405 \text{ \AA}$ ). The monochromator used was Johansson Type. The emission and excitation spectral measurements were performed with resolution increment 1 nm and slit 5 nm using Jobin-Yvon-Horiba Fluor log III fluorimeter and the Fluorescence program. The excitation source was a 100 W Xenon lamp, and the detector used was R-928 operating at a voltage of 950 V. Synchronous fluorescence scan was measured using the same instrument by keeping the excitation and emission slits width at 0 nm. Scanning electron microscopy (SEM) analysis was done using Tuscan. The thermogravimetric Analysis (TGA) was done by using a Netzsch TGA 209 in the temperature range 30°C to 1000°C with an increment of 10 K/min in a  $\text{N}_2$  atmosphere. Ultracentrifugation technique was used for separation and washing the samples.

## 2.4. Synthesis of curcumin conjugated Ag NPs



169.7 mg of crystals of silver nitrate (1.0 mol) and 184.19 mg (0.5 mol) of curcumin were mixed and grinded in a marble mortar using a pestle until the crystals crushed and turned into powder, during this period color changed from yellow to dark orange approximately (from 30 min to 60 min depending on the temperature). The powder mixture was then dissolved in 100 mL ethanol and the solution was transferred into two 50 mL tubes. The total volume of the solution was approximately 95 mL. Subsequently, growth of Ag NPs continued in ethanol for 1, 2, 4, 8, and 16 hours and for 1, 2, 3, 5, and 7 days at four different temperatures, such as 4°C, 20°C, 40°C, and 60°C. Then after incubating for the specific time mentioned above we centrifuged the tubes for 20 minutes at 4000 rpm at 20°C. To remove all the unreacted or unbounded curcumin from the solutions, the samples were washed with ethanol and centrifuged, then we discarded the solution (yellow solution). We repeated the washing part several times (around 5 times) until the supernatant was clear of all the curcumin. After finishing the washing part, we got rid of the ethanol and put water instead, like 10 mL in each tube, and stored them. We

took 1 mL of the stored sample with 3 mL of water, and characterize it by SEM, UV-VIS spectrophotometry, and fluorescence techniques.

## **2.5. Results and discussion**

The curcumin conjugate Ag NPs were prepared in the solid state chemistry by the participation of silver nitrate and curcumin as a starting material and using the curcumin as a reducing agent to reduce  $\text{Ag}^+$  in silver nitrate to  $\text{Ag}^0$ , the metallic form. Curcumin and silver nitrate were mixed in their solid state at four different temperatures 4 °C, 20 °C (room temperature), 40 °C and 60 °C, at ten different times 1, 2, 4, 8, 16 hours and 1, 2, 3, 5, and 7 days. After grinding the starting materials in their solid state the color changed from bright yellow to orange. Then we preserved the solid mixture in an organic medium which was ethanol to prevent  $\text{O}_2$  from entering the mixture and forming silver oxide and to grow the Ag NPs particles. After the period of time ends we centrifuged the sample for 20 minutes and washed it by ethanol until we got rid from all the yellow color and obtained a transparent solution. After having the transparent solution we discarded all the ethanol and added double distilled water (DDW) like 10 mL, then we stored it. Some of the Ag NPs must also be lost to the solution during washing. For SEM, UV-VIS and fluorescence studies we took 1 mL from the sample and added 3 mL DDW in a small vials, and we took the desired amount to study it in catalysis and sensing applications.

## 2.6. Characterization

### *X-ray diffraction analysis (XRD)*

The particles were collected by using the freeze drier to evaporate all the water that we used to store the samples with. The XRD pattern of curcumin conjugated Ag-NPs is shown in Figure 2. The sharp Bragg reflection in the XRD spectrum indicates the presence of organic content associated with Ag NPs. All the major peaks in XRD can be indexed for the face centered cubic structure of Ag NPs. The different peaks originated from the (1 1 1), (2 0 0), (2 2 0), and (3 1 1) planes of Ag NP, which perfectly match with the JCPDS card number 4-0783<sup>41</sup>. A major peak at lower  $2\theta$  value might be due to the organic content of curcumin. The XRD pattern further reveals that curcumin conjugated silver nanoparticles are crystalline in nature. The average diameter of silver nanoparticles can be estimated from the (111) diffraction peak using Scherrer's equation as  $L = 0.91 \lambda / (\beta \cos \alpha)^3$  where L is the mean crystallite size,  $\lambda$  the wavelength of incident rays (1.5405 Å),  $\beta$  is the full width at half maximum (FWHM) of the highest intensity peak in radians, and  $\alpha$  is the center angle of the peak in radian. The mean crystallite range for Ag NPs was determined to be 8.47 nm using this formula. This is lower than the values found in the SEM images.

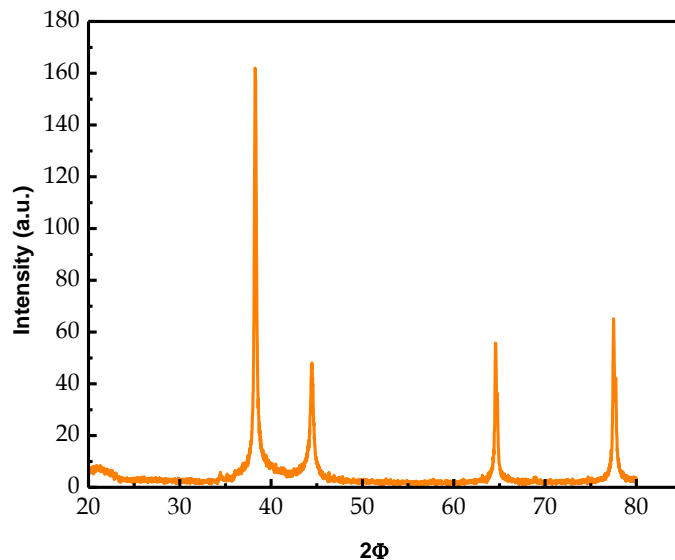


**Figure 2: XRD pattern of curcumin conjugated Ag NPs prepared after 1day at 60°C**

*Thermogravimetric analysis (TGA)*

Thermogravimetric analysis is shown in Figure 3, the Ag NPs obtained at 60°C within the one day sample. The decomposition temperature for curcumin from literature is approximately at 400 °C and sometimes at 200 °C<sup>42</sup>, so it has a wide range of decomposition temperatures. In Figure 3 we can see a wide range of decomposition temperature started at approximately 250 °C till 600 °C which is the same range as curcumin decomposes temperatures with a weight lose mass of the organic compound approximately ~8%. This indicates the presence of only silver nanoparticles in our sample, and that all the AgNO<sub>3</sub> reacted with curcumin and formed Ag NPs.



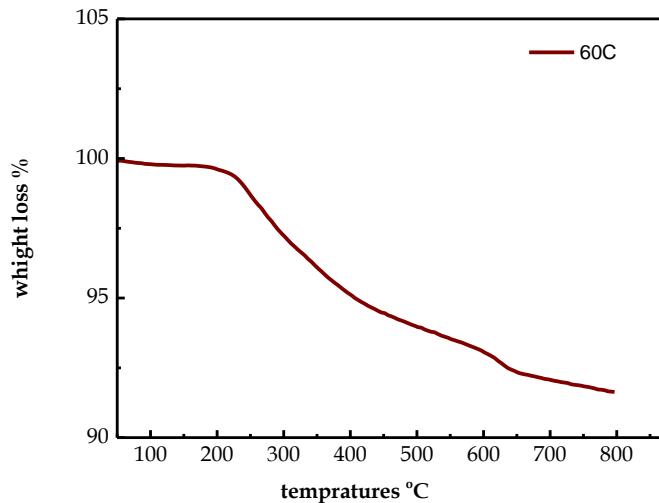
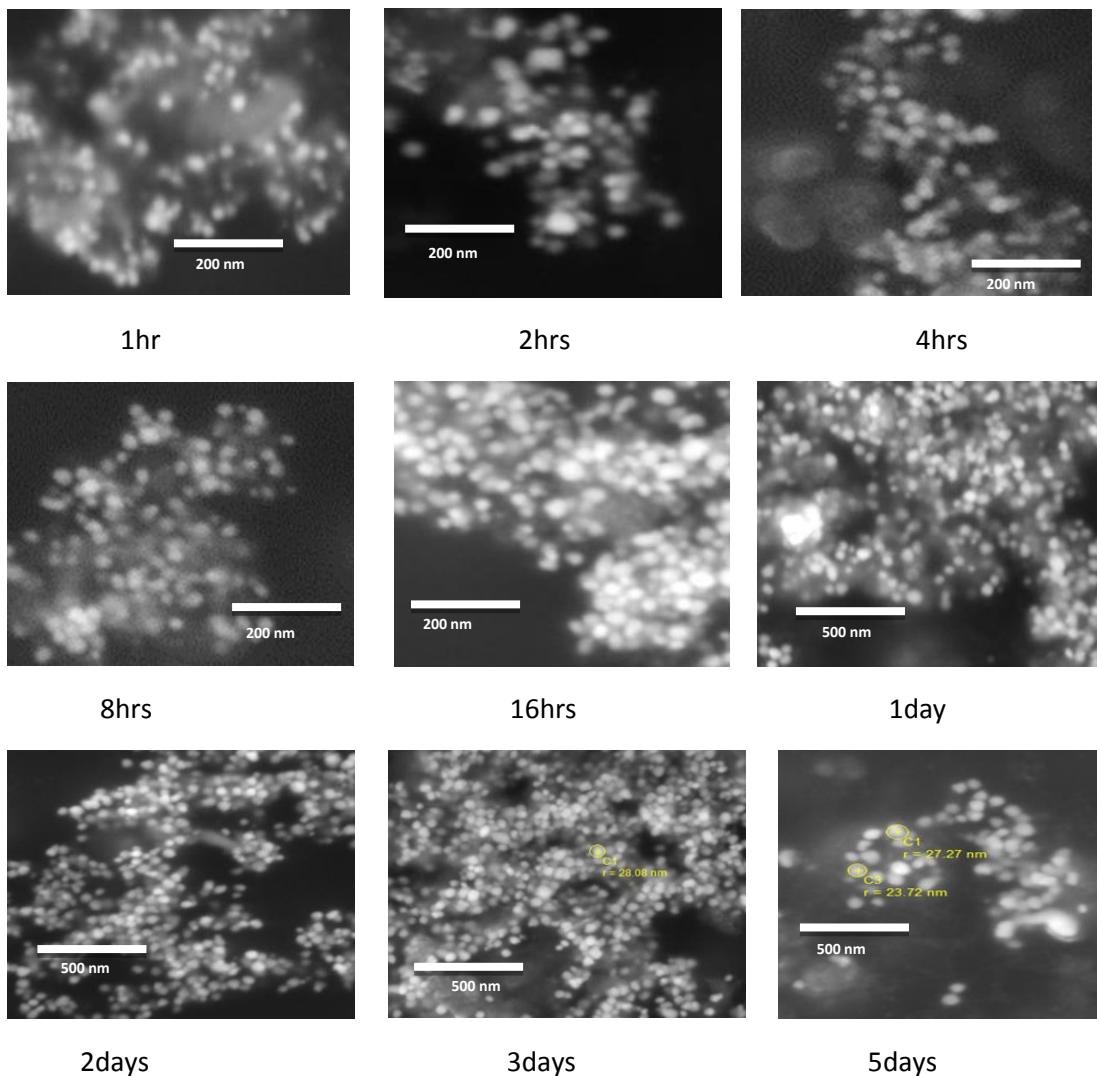


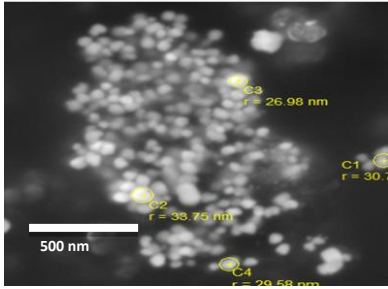
**Figure 3: TGA of the curcumin conjugated Ag NPs sample prepared at 60°C and grown for 1 day**

*Scanning electron microscopy (SEM)*

The SEM images recorded mostly in 500 nm resolution, show variation in the size of Ag NPs for the ten different times at the four different temperatures. Figure 4 at 4°C shows how the particles became bigger with increase in growth time at the same temperatures. The 1 hour growth sample shows a very small particle size for which we could not measure the radius, but from one day till seven days growth samples the particles size diameter ranged between 15 and 40 nm, and there were particles having smaller size with mostly a spherical shape. At 20°C shown in Figure 5 the particles became bigger with more variety in shapes like spherical and hexagonal shapes. The particles size of the 1 hour growth sample are very small in such a way that we could not measure the particles diameter. From one day till seven days samples, the size ranged between 40 and 90 nm, in this case the particles shapes were spherical, hexagonal and we noticed formation of rod-shaped particles. At 40°C, given in Figure 6, the size of the particles ranged between 20 and 100 nm. More variety in particles shapes spherical, hexagonal and rods shapes

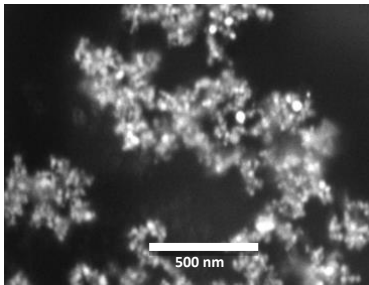
were found. Figure 7 presents the ten samples at 60°C, in this case the particles size were bigger and the size ranged from 30 to 130 nm, the shapes are mostly hexagonal with spheres and rods shapes. At all four temperatures under investigation, we could see a good amount of particle aggregation. With different sizes and shapes in each sample, also many of the SEM pictures show imperfection, some blurriness or unclear images due to the presence of unreacted curcumin in the sample. During the sample preparation, we noticed there was a change in sample color from light yellow in the one hour growth sample to dark yellow or orange in the seven days growth sample.



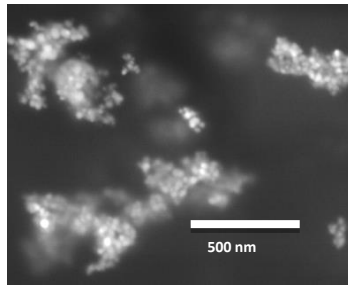


7days

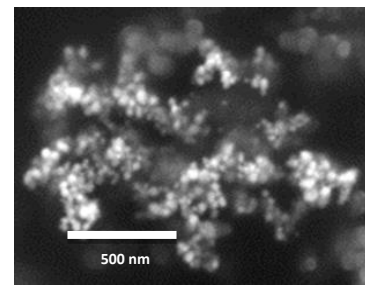
**Figure 4: SEM images of curcumin conjugated Ag NPs in different growth time intervals at 4°C.**



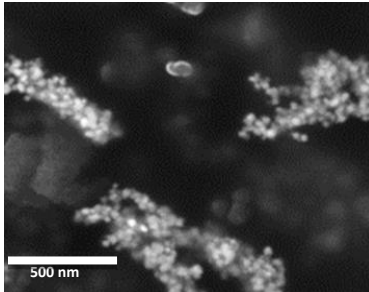
1hr



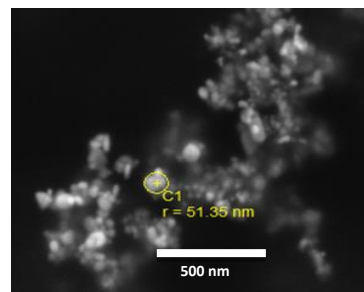
2hrs



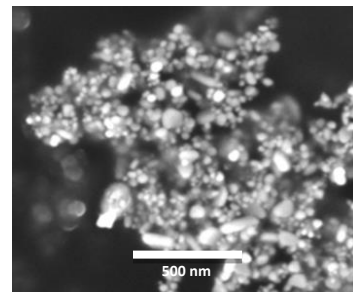
4hrs



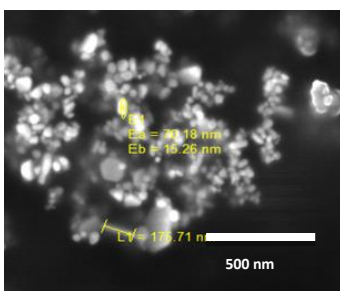
8hrs



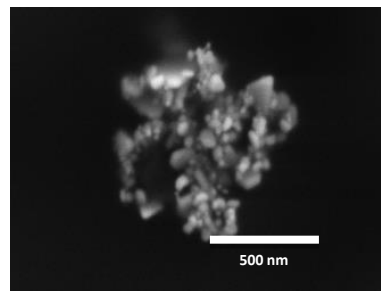
16hrs



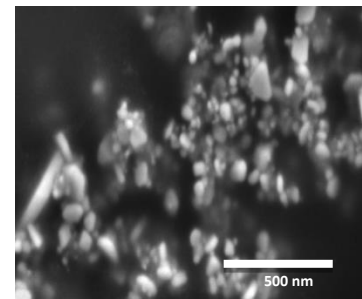
1day



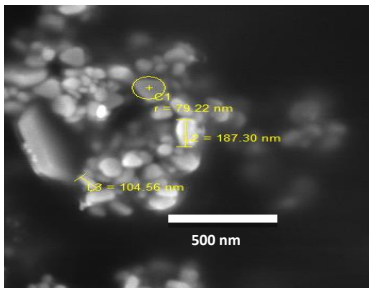
2days



3days

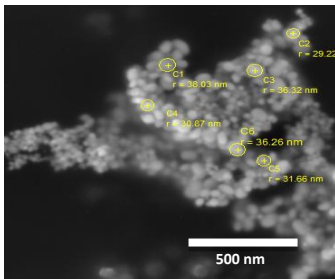


5days

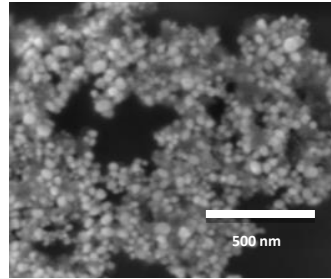


7days

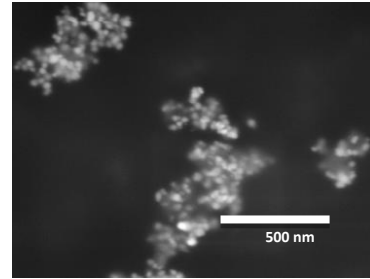
**Figure 5: SEM images of curcumin conjugated Ag NPs in different growth time intervals at 20°C.**



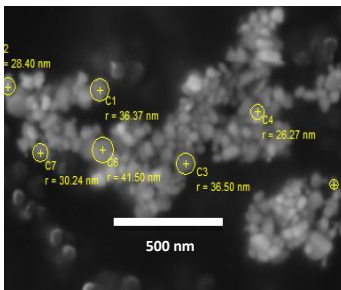
1hr



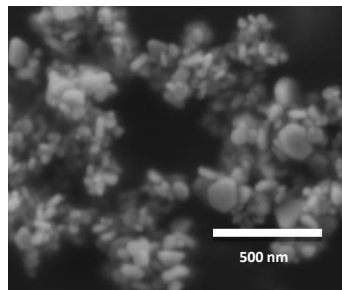
2hrs



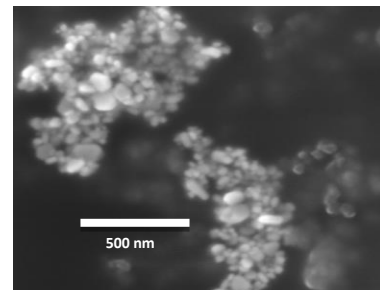
4hrs



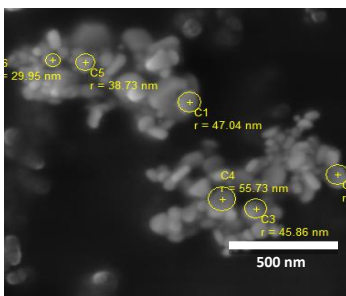
8hrs



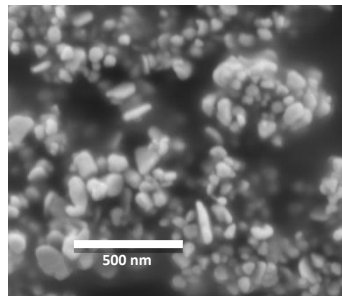
16hrs



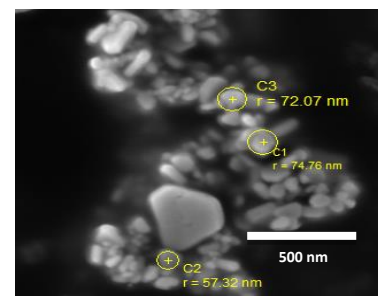
1day



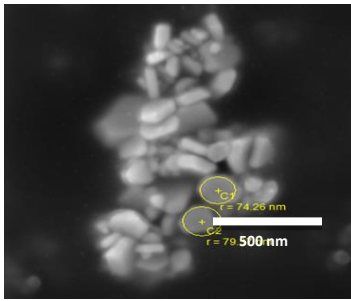
2days



3days

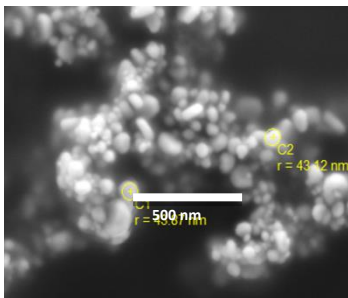


5days

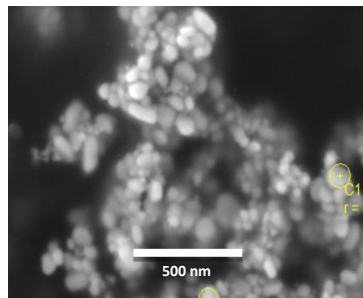


7days

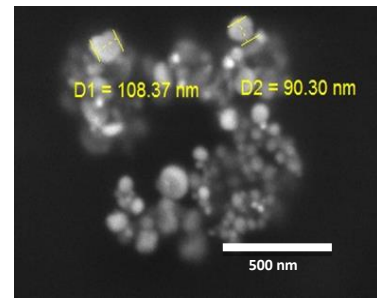
**Figure 6: SEM images of curcumin conjugated Ag NPs in different growth time intervals at 40°C.**



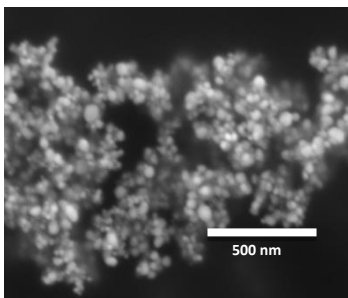
1hr



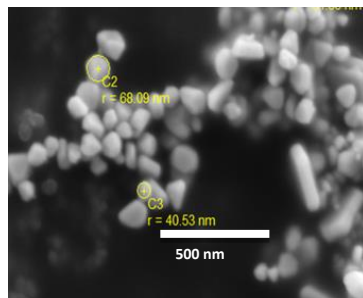
2hrs



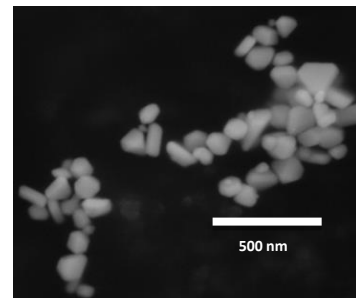
4hrs



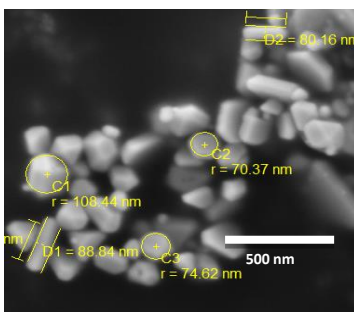
8hrs



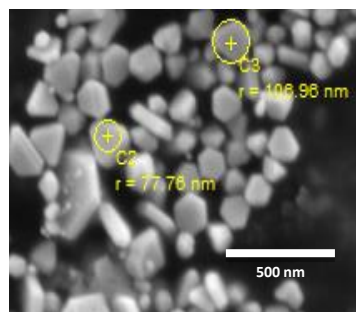
16hrs



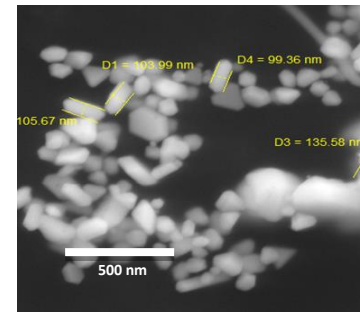
1day



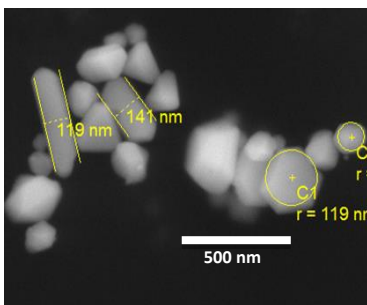
2days



3days



5days



7days

**Figure 7: SEM images of curcumin conjugated Ag NPs in different growth time intervals at 60°C.**

## 2.7. Spectroscopic measurement

### *UV-VIS spectroscopy*

The UV-visible spectra obtained for the four different temperatures at ten different growth times is given in Figure 8. We noticed different peaks and intensities for the different growth time samples due to the different sizes and shapes. Curcumin strongly absorbs at around 266 nm for  $S_1 - S_2$  transition and at around 425 nm for  $S_0 - S_1$  transition in aqueous medium<sup>43</sup>. However, the mixture of curcumin and  $AgNO_3$  that was used to prepare Ag NPs showed absorbance peaks around 440-450 nm in all temperatures and as the reaction time increased, the peaks shifted to 500 nm. Sharp peaks were noticed at 250 nm for 4°C and 20°C whereas for 40°C and 60°C it shifted to a higher wavelength, this is due to  $Ag^+$  bounded to curcumin<sup>44</sup>. Curcumin has the ability to chelate on the cation metals like  $Zn^{+2}$  and  $Cu^{+2}$  (M-L) whereby those cations will bind to C=O group of the  $\beta$ -diketone moiety on curcumin<sup>45</sup>. The absorbance peaks for Ag NPs appear because of the elastic scattering phenomenon as a result of Surface Plasmon resonance (SPR).



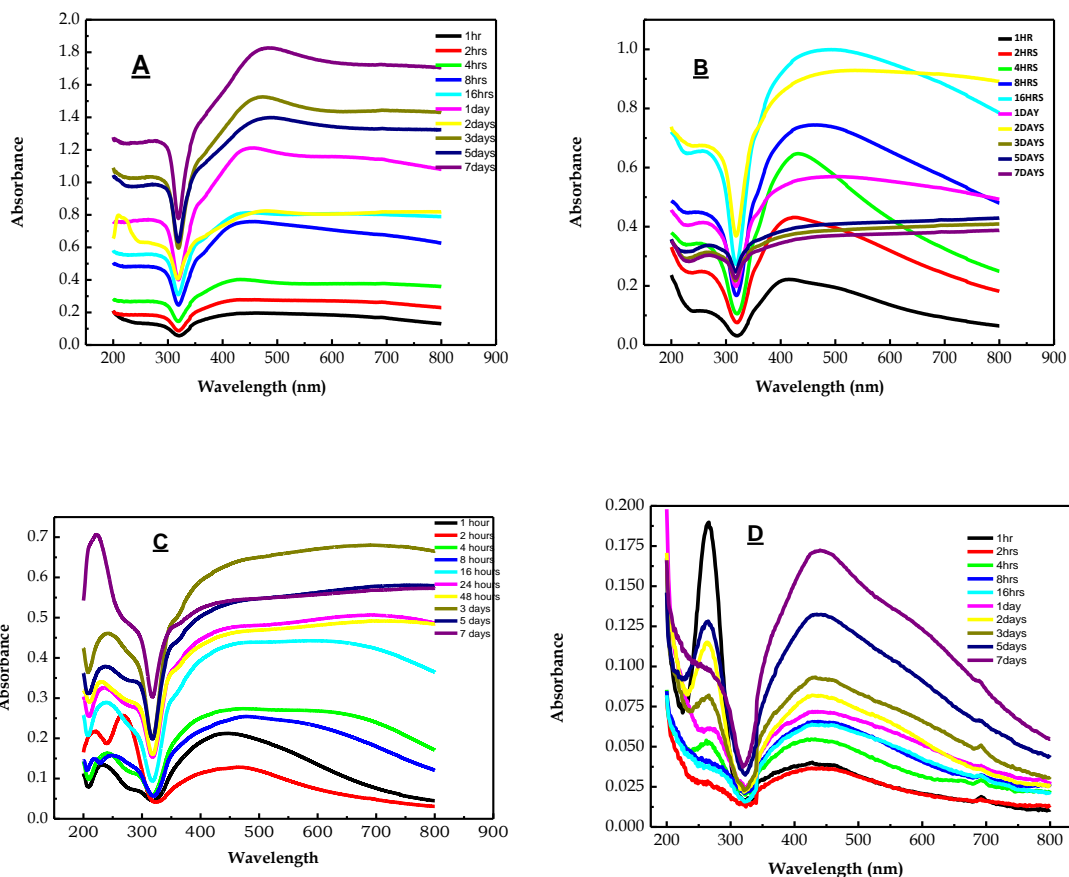


**Figure 8: UV-VIS spectra of curcumin conjugated Ag NPs prepared at different growth time intervals for four different temperatures, (A) 60°C; (B) 40°C; (C) 20°C and (D) 4°C.**

With the 1, 2, 3, 5, 7 days growth samples the peak position shifted to higher wavelength than the 1, 2, 4, 8, 16 hours growth samples due to bigger size of the particles. Also when we did a comparison by keeping the time fixed and changing the temperature only, as shown in Figure 9A and B, it was observed that at higher temperature, which was 60 °C in this case, the peak shifted to higher wavelength than 40°C, 20°C and 4°C. This happened because with higher temperature larger size particles are formed, which shift the absorption to the longer wavelength. Ag NPs prepared at 60°C gave bigger particles

than 40°C. 20°C gave bigger particles than 4°C, as shown in the SEM images presented in Figures 4, 5, 6 and 7.

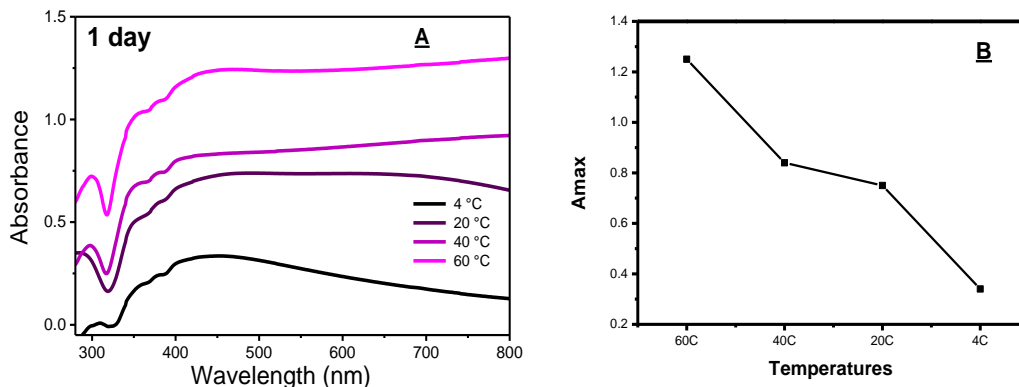


**Figure 9: A) UV-VIS spectra of curcumin conjugated Ag NPs at the four different temperatures in one day growth sample. B) Absorbance ( $A_{\max}$ ) vs temperatures for one day growth sample.**

#### *Fluorescence spectroscopy*

The fluorescence spectra of curcumin conjugated silver nanoparticles were recorded with an excitation wavelength of 425 nm, and fluorescence emission range was kept in 440 - 600 nm as in most the solvent environment curcumin emits in this range<sup>46,47</sup>. In a pure solution of curcumin in polar solvent like water, a broad peak maximum at ~550 nm appears in the emission spectra<sup>9,44</sup>, whereas in the present sample of curcumin conjugated Ag NPs only one strong peak appeared at ~490 nm in water as shown in Figure 10, this means that all the curcumin reacted with AgNO<sub>3</sub> and formed curcumin conjugated Ag NPs.



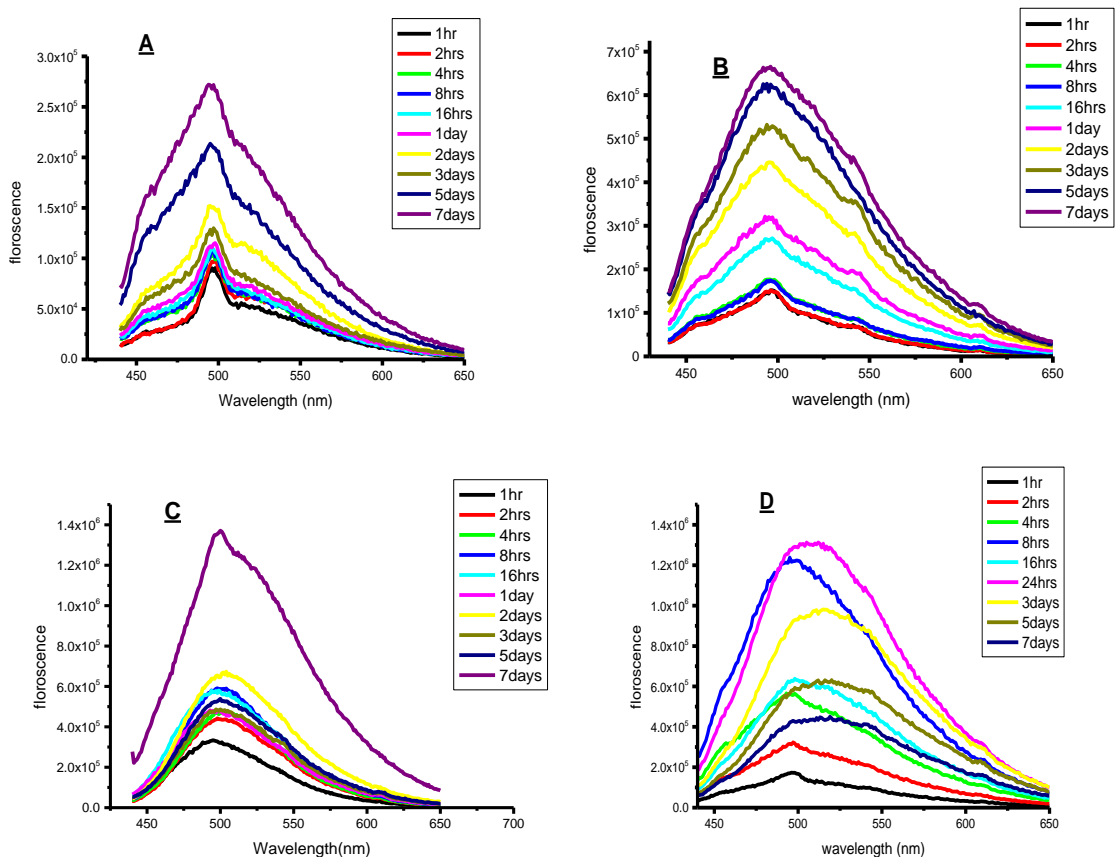


**Figure 10: Fluorescence emission spectra of curcumin conjugated Ag NPs in different growth time intervals at 425 nm excitation wavelength, (A) 4°C; (B) 20°C; (C) 40°C and (D) 60°C.**

It was found that the intensity of fluorescence increased with time indicating bigger particles have higher fluorescence intensities, as shown in Figure 11, suggesting more amount of curcumin conjugation for the given amount of Ag NPs. This is logical since the nucleation of Ag NPs occurs to form larger particles, curcumin conjugation occurs only at the surfaces.

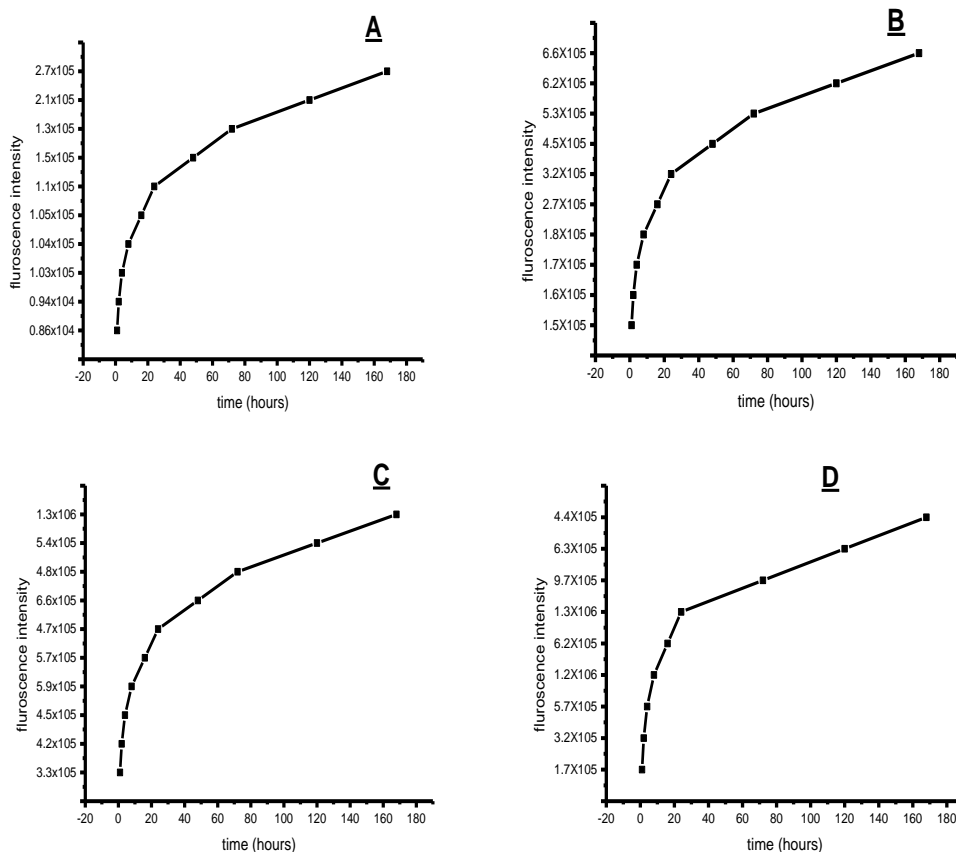


**Figure 11: Fluorescence emission intensity at the maximum vs growth time in hours for curcumin conjugated Ag NPs at 425 nm excitation wavelength, (A) 4°C; (B) 20°C; (C) 40°C and (D) 60°C.**

The Resonance Rayleigh Scattering (RRS) spectra as shown in Figure 12 was measured by applying synchronous fluorescence scan method by keeping the wavelength interval ( $\Delta\lambda$ ) at 0 nm. The Resonance Rayleigh Scattering spectrum of curcumin conjugated Ag NPs at four different temperatures with ten different growth times showed four bands. The first two bands are the due to excitation bands which is similar to what we have in UV-VIS spectra in Figure 8, and the other two bands are around emission region of curcumin conjugated Ag NPs particles. As expected bigger particles have higher SFS or RRS intensity and the wavelength shifts to longer wavelength. Also when the

temperature increased, the SFS intensity increased from  $2.5 \times 10^8$  in  $4^\circ\text{C}$  till  $8.5 \times 10^8$  in  $60^\circ\text{C}$  for the longer wavelength band, thus, the position of the wavelength maximum increased from 600 nm till 750 nm as shown in Figure 12 A, B, C and D.

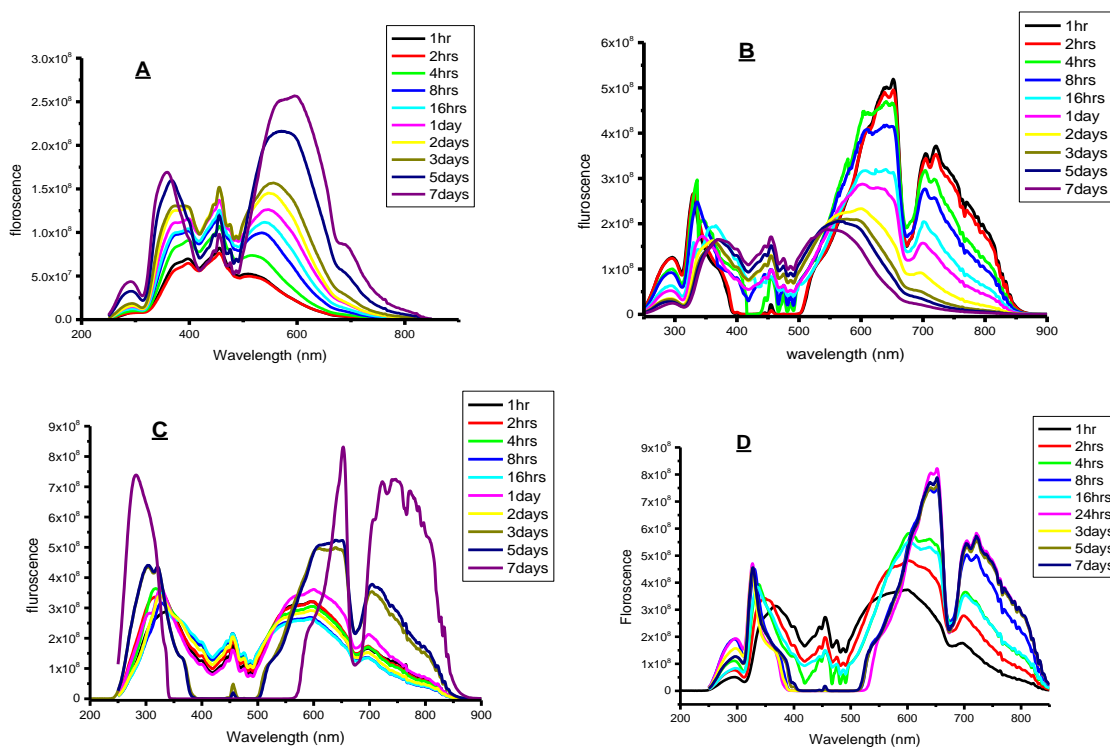
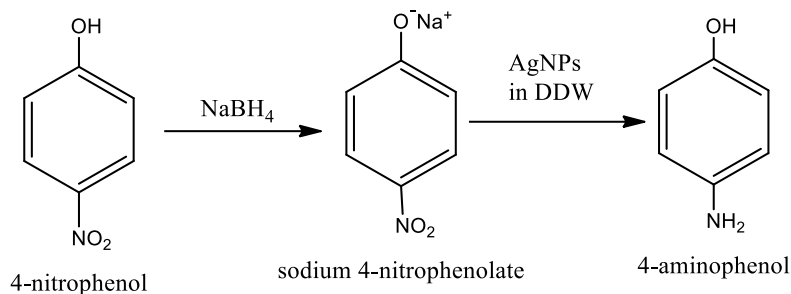


**Figure 12: Synchronous fluorescence spectra of curcumin conjugated Ag NPs in different growth time intervals at 425 nm excitation wavelength, (A)  $4^\circ\text{C}$ ; (B)  $20^\circ\text{C}$ ; (C)  $40^\circ\text{C}$  and (D)  $60^\circ\text{C}$ .**

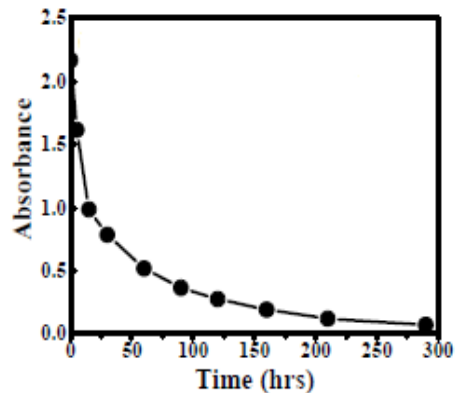
## 2.8. Catalytic study

One of the important applications of silver nanoparticles (Ag NPs) is that they are used as nano-catalysts for the reduction of 4-nitrophenol with  $\text{NaBH}_4$  (nitro-reduction). 500 microliters (0.5 ml) of curcumin conjugated Ag NPs was added to 15 mM of  $\text{NaBH}_4$  that was prepared instantly, then they were mixed together with 0.15 mM of 4-nitrophenol, the total volume was equal to 3 mL. The initial color of the mixture was yellow, then it

turned to transparent solution because of the reduction 4-nitrophenol to 4-aminophenol, after the addition of  $\text{NaBH}_4$ . The reduction reaction is given below:

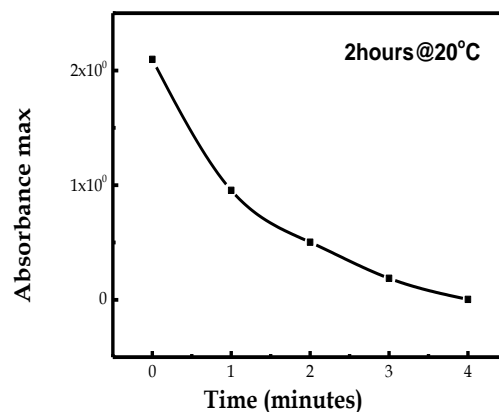
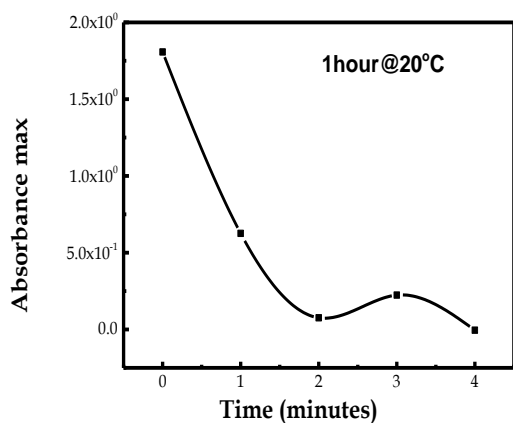


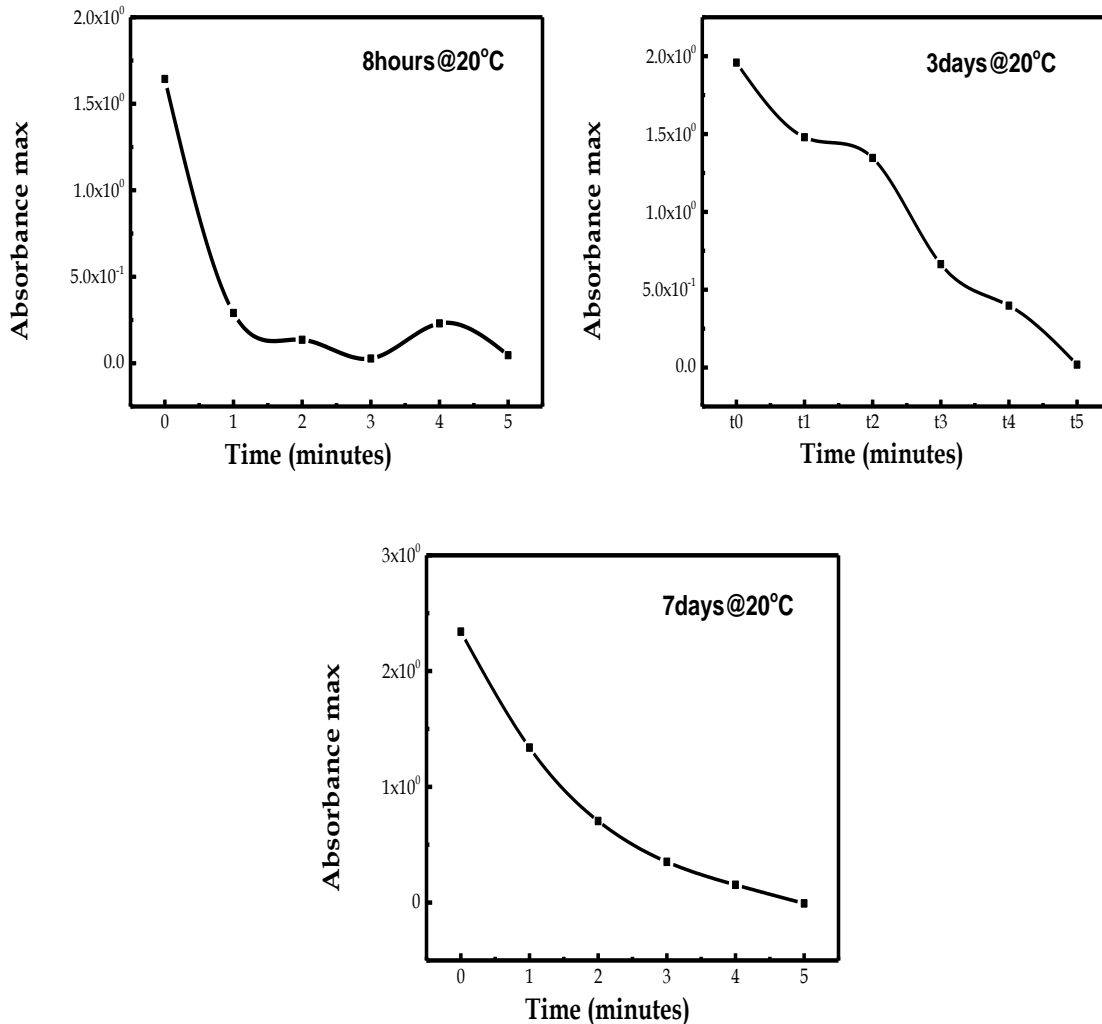
The reduction of 4-nitrophenol was observed by measuring the change in the absorbance of 4-nitrophenol at 400 nm, and to confirm that this reduction happens a peak at 290 nm was also identified for the 4-aminophenol<sup>48</sup>. To study the effect of the curcumin conjugated Ag NPs as a catalyst on the reduction of 4-nitrophenol to 4-aminophenol, first we measured the absorbance of the reduction of 4-nitrophenol by using UV-VIS spectra without curcumin conjugated Ag NPs, and then we measured the reduction reaction in the presence of curcumin conjugated Ag NPs. In the first reaction, the absorbance of 4-nitrophenol at 400 nm decreased with time, and for complete reduction we need approximately 300 hours as shown Figure 13.



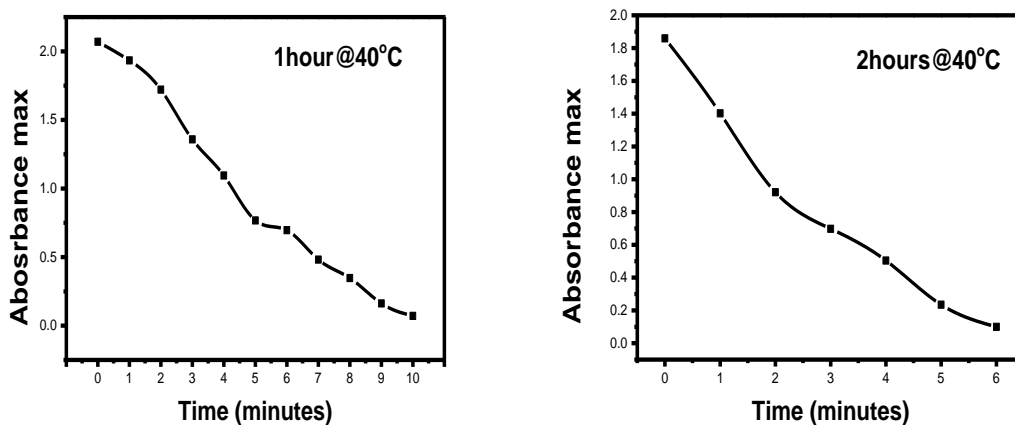
**Figure 13: Change in the absorbance of 4-nitrophenol at ~400 nm in the presence of NaBH<sub>4</sub> without Ag NPs<sup>43</sup>**

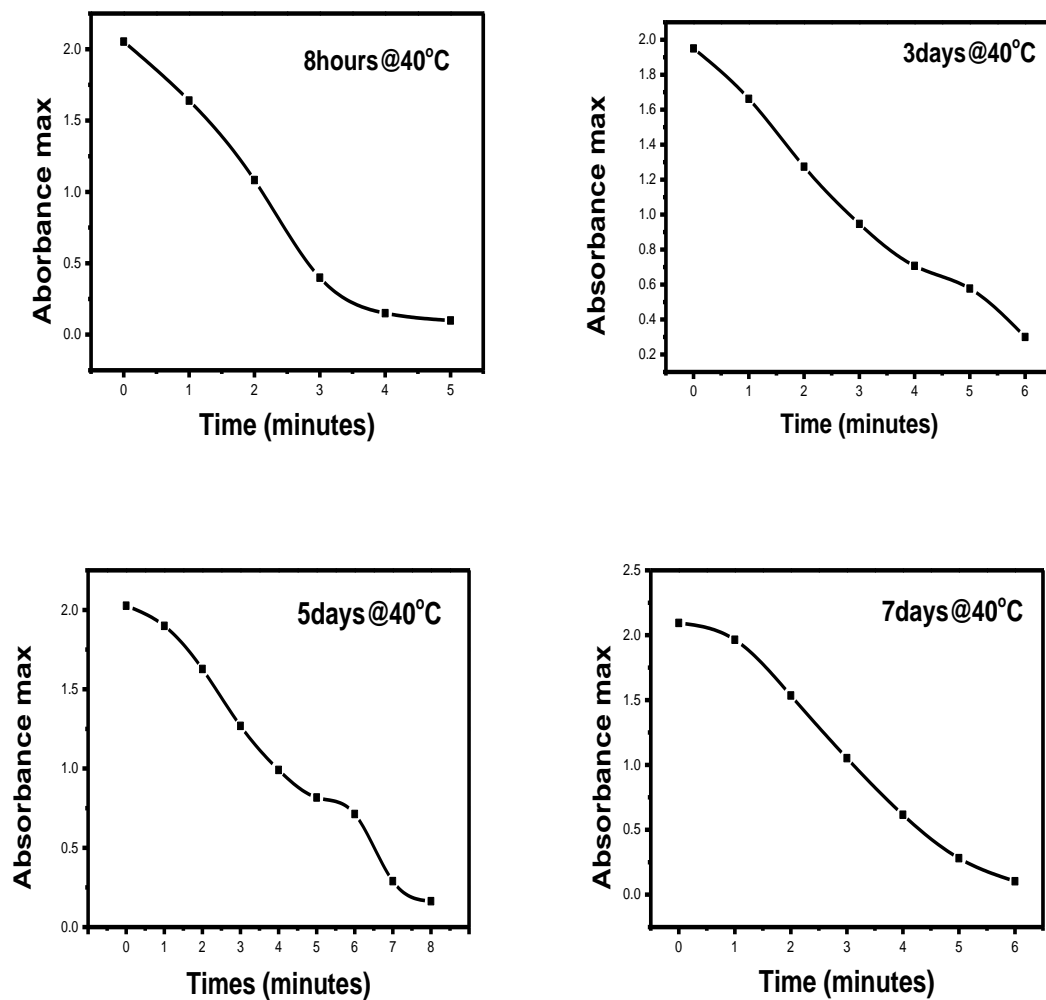
In the second reaction absorbance of 4-nitrophenol at 400 nm was monitored in the presence of curcumin conjugated Ag NPs with time, it was found that in the presence of curcumin conjugated Ag NPs 4-nitrophenol reduced within a few minutes (12 minutes maximum) as shown in Figures 14, 15, and 16. This is because curcumin conjugated Ag NPs will adsorb sodium borohydride and make the reduction of 4-nitrophenol to 4-aminophenol faster.



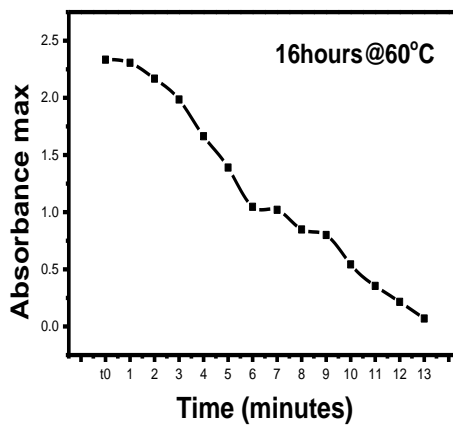
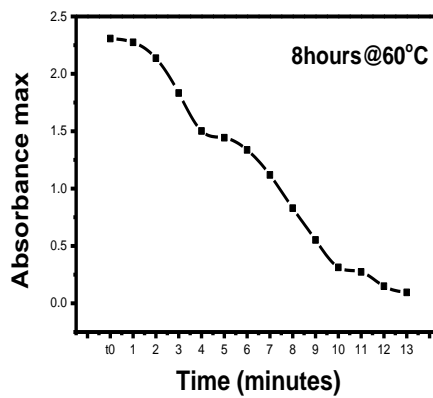
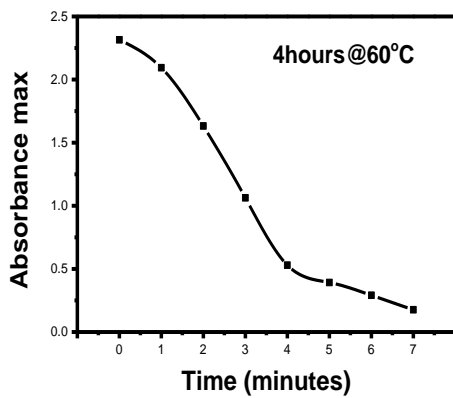
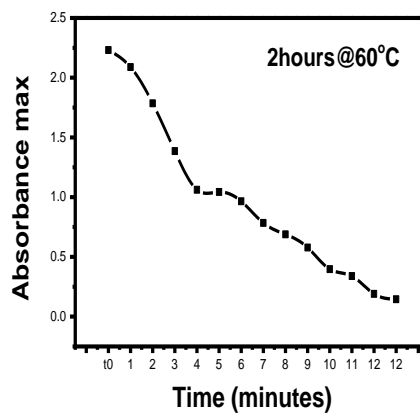
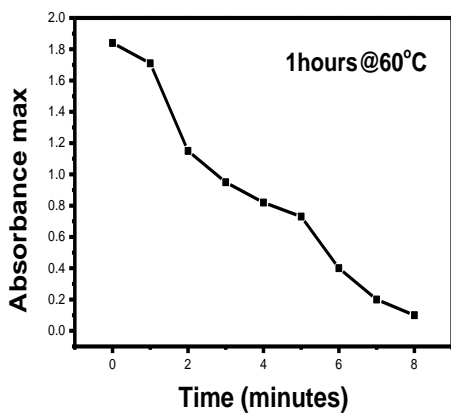


**Figure 14: Change in the absorbance of 4-nitrophenol at ~400 nm in the presence of NaBH<sub>4</sub> with curcumin conjugated Ag NPs prepared in different growth times at 20°C.**





**Figure 15: Change in the absorption of 4-nitrophenol at ~400 nm in the presence of NaBH<sub>4</sub> with curcumin conjugated Ag NPs prepared in different growth times at 40°C.**





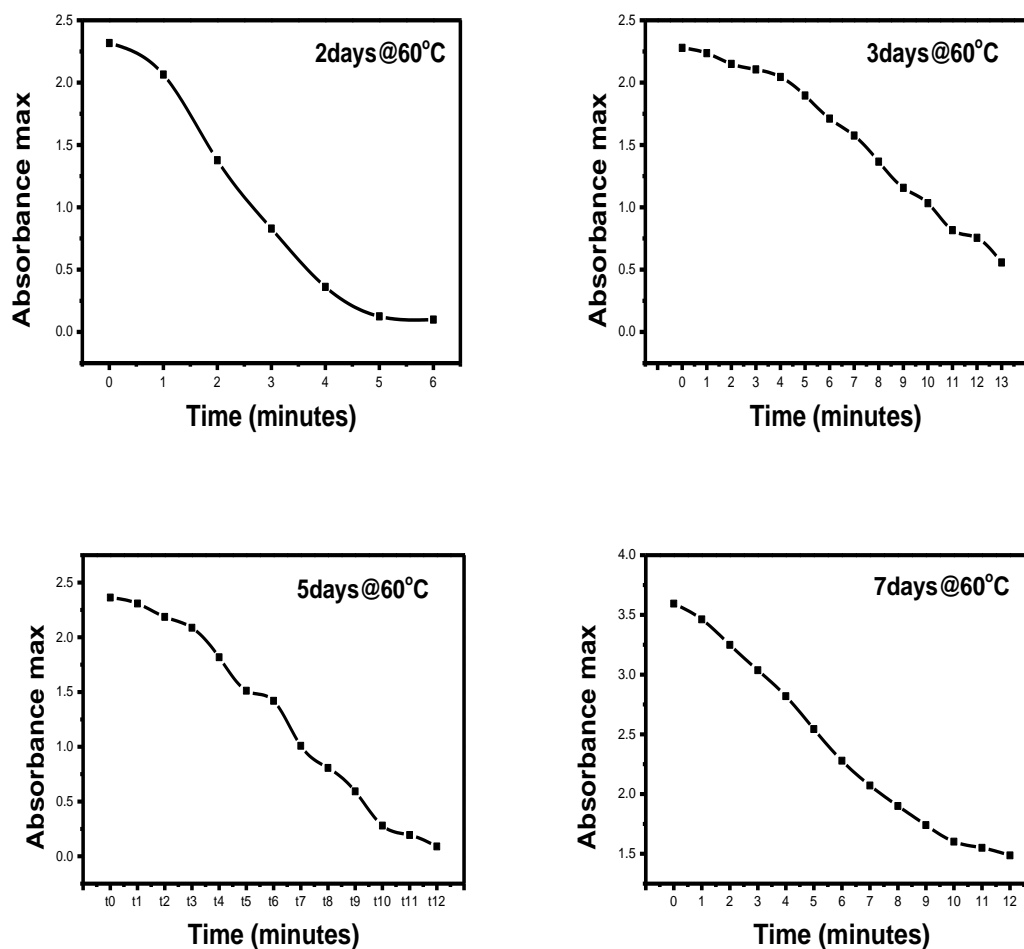


**Figure 16: Change in the absorbance of 4-nitrophenol at ~400 nm in the presence of NaBH<sub>4</sub> with curcumin conjugated Ag NPs prepared in different time at 60°C.**

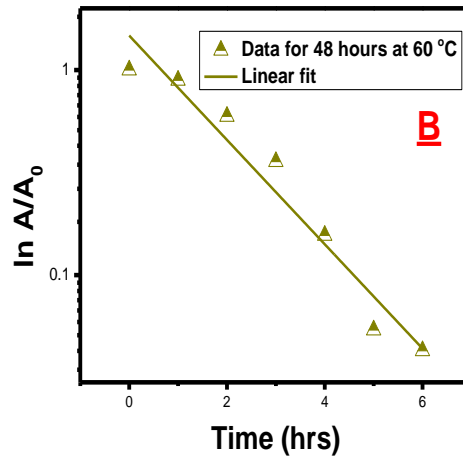
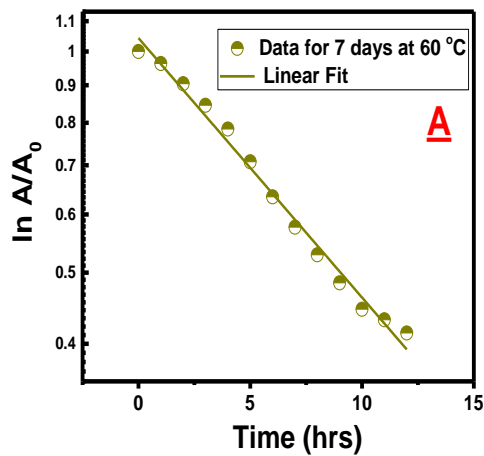
Therefore, curcumin conjugated Ag NPs prepared at the different temperatures at ten different growth times can be excellent catalysts for the reduction of 4-nitrophenol.

However, different size and shape of Ag NPs were obtained at different temperatures, 20 °C, 40 °C, 60 °C, and for ten different growth times, therefore, the catalytic activities were compared for Ag NPs that were prepared in different temperatures at ten different growth times. The catalysis reaction considered to be pseudo first rate reaction because of

the decreasing in intensity of the absorption peak at 400 nm over time, so a linear relation was observed between  $\ln (A/A_0)$  vs. time, but the concentration of sodium borohydride considered to be constant. The equation below represent the linear relationship between  $\ln (A/A_0)$  and time:

$$\ln (A/A_0) = - \kappa t$$

Where  $A_0$  is the initial absorbance of the reaction system,  $A$  is the absorbance at time  $t$ , and  $\kappa$  is the rate constant of the chemical reduction (see Appendix 1). From this kinetic curve, the rate constant  $\kappa$  ( $s^{-1}$ ) was calculated and it shows that 7 days growth time at  $60^\circ\text{C}$  has lower  $\kappa$  which is equal to  $0.035\text{ s}^{-1}$  as shown in Figures 17, 18 and 19.



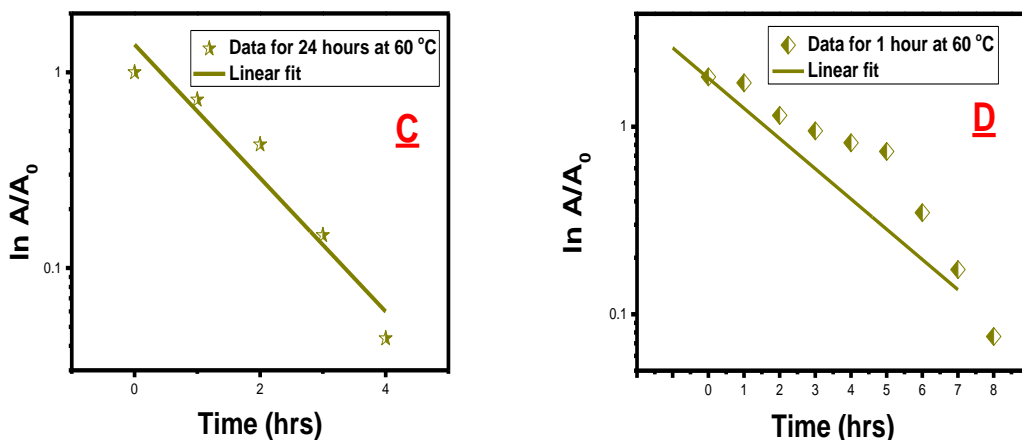


**Figure 17:** Change in  $\ln(A/A_0)$  with time during reduction of 4-nitrophenol in the presence of  $\text{NaBH}_4$  with curcumin conjugated Ag NPs prepared at four different growth times at 60°C; (A) 7 days growth time,  $\kappa = 0.035 \text{ s}^{-1}$ ; (B) 2 days growth time,  $\kappa = 0.254 \text{ s}^{-1}$ ; (C) 1 day growth time,  $\kappa = 0.341 \text{ s}^{-1}$ ; and (D) 1 hour growth time,  $\kappa = 0.161 \text{ s}^{-1}$ .

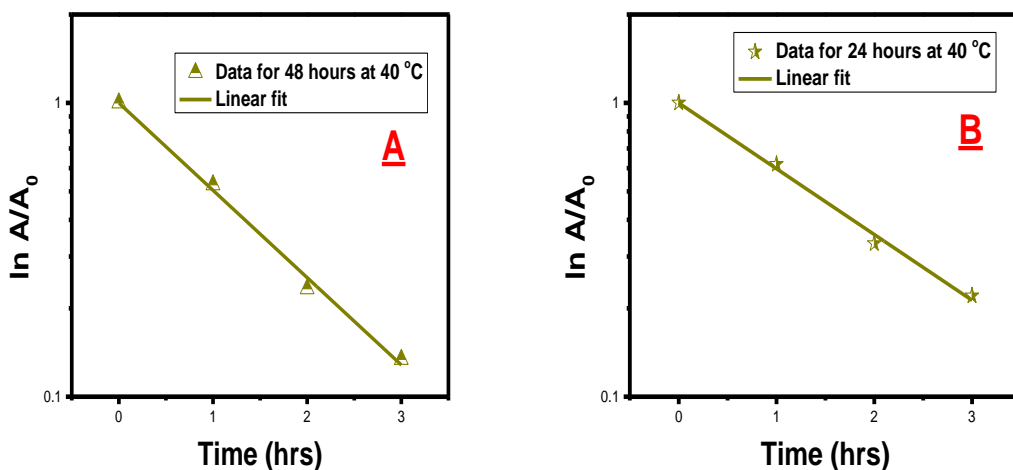


**Figure 18:** Change in  $\ln(A/A_0)$  with time during reduction of 4-nitrophenol in the presence of  $\text{NaBH}_4$  with curcumin conjugated Ag NPs prepared at two different growth times at 40°C; (A) 2 days growth time,  $\kappa = 0.297 \text{ s}^{-1}$  and (B) 1 day growth time,  $\kappa = 0.224 \text{ s}^{-1}$ .

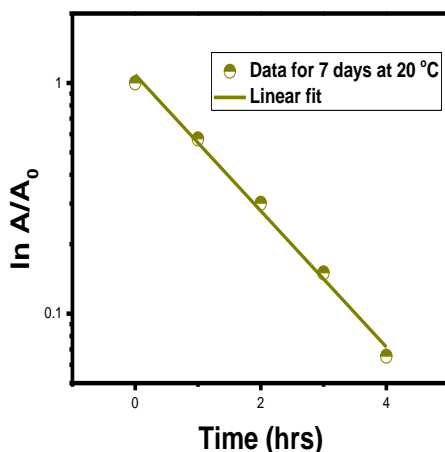


**Figure 19: Change in  $\ln (A/A_0)$  with time during reduction of 4-nitrophenol in the presence of  $\text{NaBH}_4$  with curcumin conjugated Ag NPs prepared at 7 days growth time at  $20^\circ\text{C}$ ,  $\kappa = 0.294 \text{ s}^{-1}$ .**

For further investigation we found that curcumin conjugated Ag NPs prepared in  $20^\circ\text{C}$  served as excellent catalysts for the reduction of 4-nitrophenol based on half life period. The half-life period was calculated as below:

$$t_{1/2} = 0.693 / \kappa$$

It shows that  $20^\circ\text{C}$  have the lowest  $t_{1/2}$  and  $60^\circ\text{C}$  have the highest  $t_{1/2}$  as depicted in Figure 20. This enhancement must be due to the different shape and size of Ag NPs in the different temperatures and growth times like we observed in the SEM images depicted in Figures 4, 5, 6, and 7, and from those Figures we can see that samples prepared at  $20^\circ\text{C}$  have in general smaller particles compared to that prepared at  $40^\circ\text{C}$  and  $60^\circ\text{C}$ , smaller size also suggests higher surface to volume ratio of the particles (see Appendix 2).

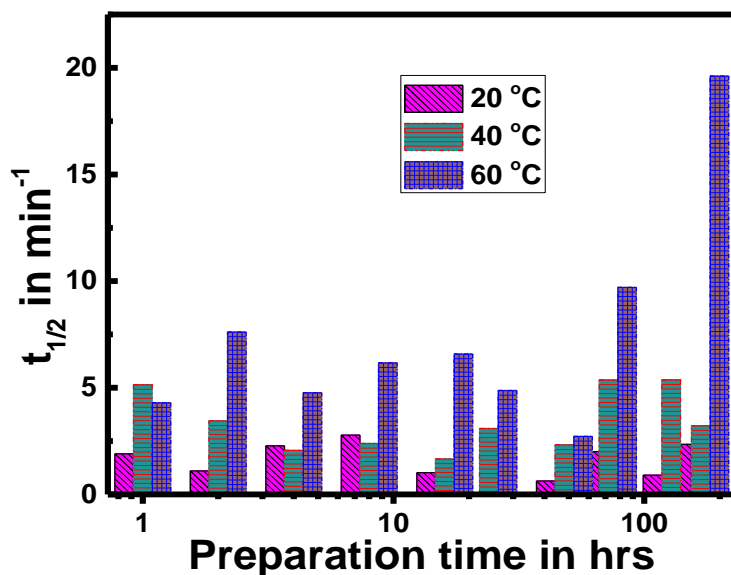
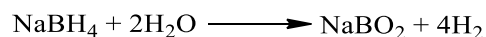
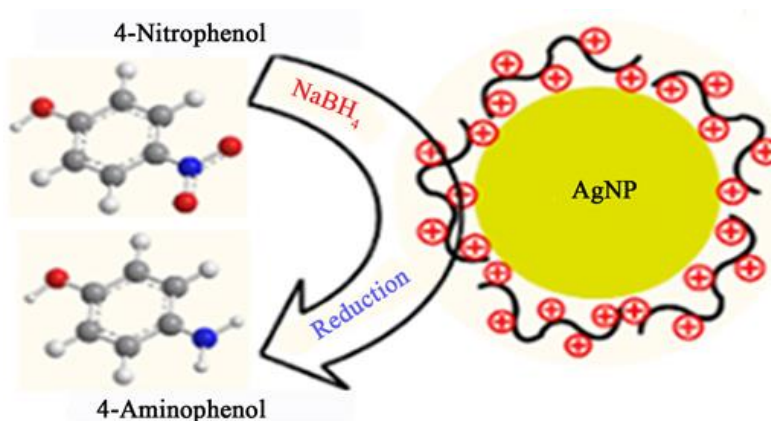


**Figure 20: Change in  $t_{1/2}$  with the growth (preparation) times at four different temperatures, 20°C, 40°C and 60°C.**

From different reviews of the literature it has been agreed that the reduction of 4-nitrophenol to 4-aminophenol in the presence of  $\text{NaBH}_4$  was held on the surface of the Ag NPs, and that Ag NPs adsorb the  $\text{H}_2$ , the hydrogen ( $\text{H}_2$ ) is released when  $\text{NaBH}_4$  reduces water to hydrogen like the equation:



Curcumin conjugated Ag NPs act as a hydrogen carrier and the H will be transported from  $\text{NaBH}_4$  to 4-NP. Then the molecules of 4-NP lose electrons, to form 4-aminophenol then the latter will desorb from the surface of curcumin conjugated Ag NPs surface as shown in Scheme 3<sup>48</sup>.

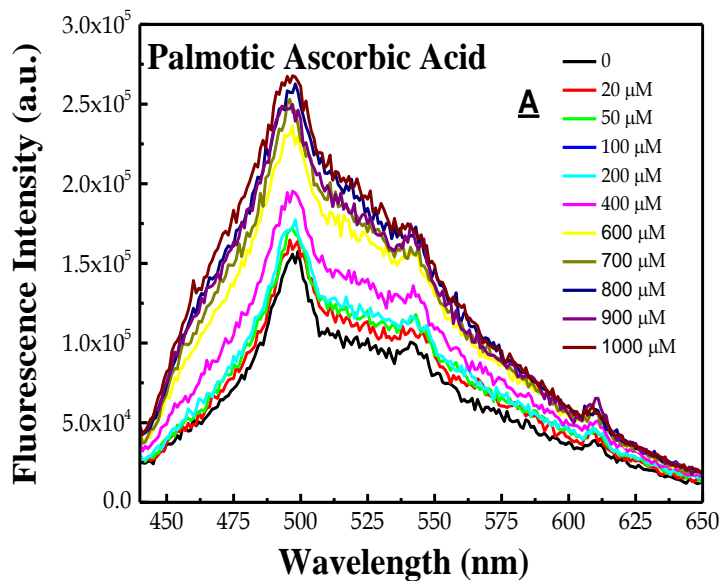


**Scheme 3: The mechanism of Ag NPs as catalyst during reduction reaction for 4-NP.**

## 2.9. Testing sensing activity

Curcumin conjugated Ag NPs can be used in bio-sensing applications by coupling or binding to the analyte, and we can record a target binding by taking note of the change in the parameters of their Resonance Rayleigh Scattering (RRS), or fluorescence signal. When the analyte interacts with the probe, the intensity of RRS/fluorescence signal will greatly increase. This is a simple technique that has been successfully used in bio sensing by nanoparticles earlier <sup>49</sup>. In this work, we tested to determine 6-O-palmitoyl-L-ascorbic acid, uric acid, oleic acid and ascorbic acid by curcumin conjugated Ag NPs. Figure 21A shows the emission spectra of curcumin conjugated silver nanoparticles in the absence and presence of 6-O-palmitoyl-L-ascorbic acid. Curcumin conjugated Ag NPs have an emission at 440-600 nm at excitation wavelength 425 nm, as mentioned earlier. Upon binding of 6-O-palmitoyl-L-ascorbic acid, the fluorescence intensity of curcumin conjugated silver

nanoparticles enhanced remarkably, but the spectral position was slightly altered. With increasing 6-O-palmitoyl-L-ascorbic acid concentration (from 20 $\mu$ M-1000 $\mu$ M) the fluorescence intensity of curcumin conjugated silver nanoparticles increased accordingly. A higher concentration yielded a higher fluorescence intensity. The calibration curve as depicted in Figure 21B showed a regular change in fluorescence intensity vs. 6-O-palmitoyl-L-ascorbic acid concentration, and could be easily apply for quantifying unknown 6-O-palmitoyl-L-ascorbic acid samples. When comparing emission spectra and sensing spectra we can see there is an increase in the intensity of the spectra and no shift in the emission wavelength when the concentration of 6-O-palmitoyl-L-ascorbic acid is increased; this is due to forming a complex between Ag NPs and 6-O-palmitoyl-L-ascorbic acid.



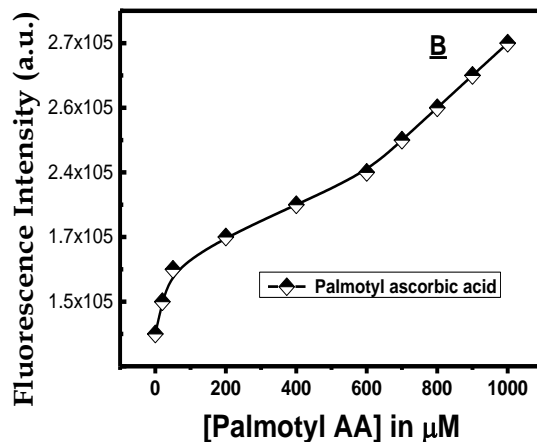


**Figure 21: A) Fluorescence emission spectra of curcumin conjugated Ag NPs with different concentration of 6-O-palmitoyl-L-ascorbic acid, B) Alteration of fluorescence intensity of curcumin conjugated Ag NPs with different concentration of 6-O-palmitoyl-L-ascorbic acid.**

When curcumin conjugated Ag NPs was tested for determining ascorbic acid having different concentration from 0 to 13 $\mu\text{M}$ , we didn't observe any change in the fluorescence intensities, which means no complexation were formed (see Figure 22).

Also the same thing with oleic acid and uric acid, no change was observed in the fluorescence intensity as shown in Figure 23 and 24. Therefore, curcumin conjugated Ag NPs can selectively determine 6-O-palmitoyl-L-ascorbic acid.

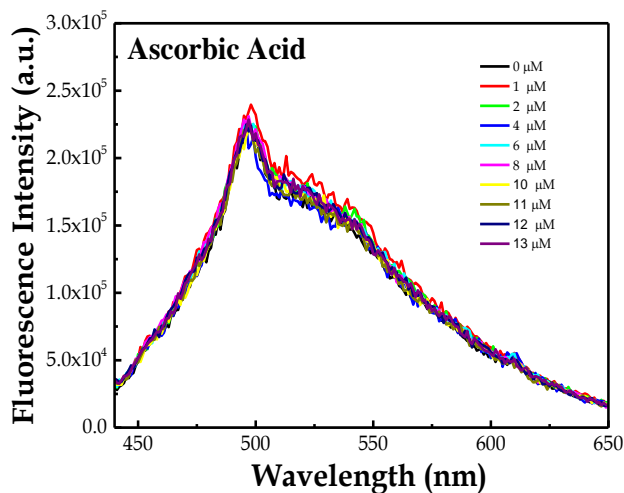




**Figure 22: Fluorescence emission spectra of curcumin conjugated Ag NPs with different concentrations of ascorbic acid.**

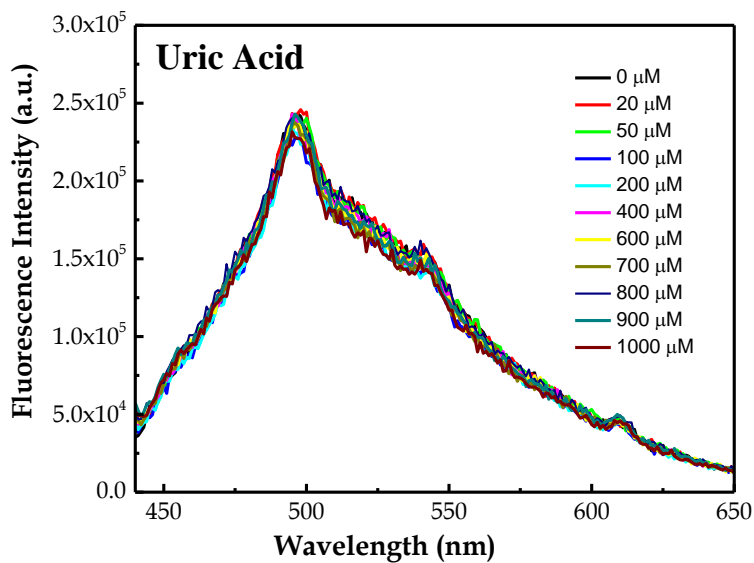


**Figure 23: Fluorescence emission spectra of curcumin conjugated Ag NPs with different concentrations of uric acid.**

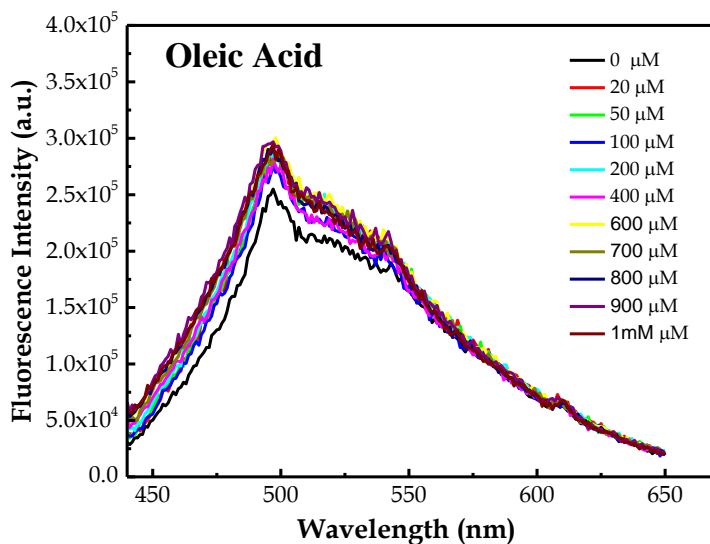


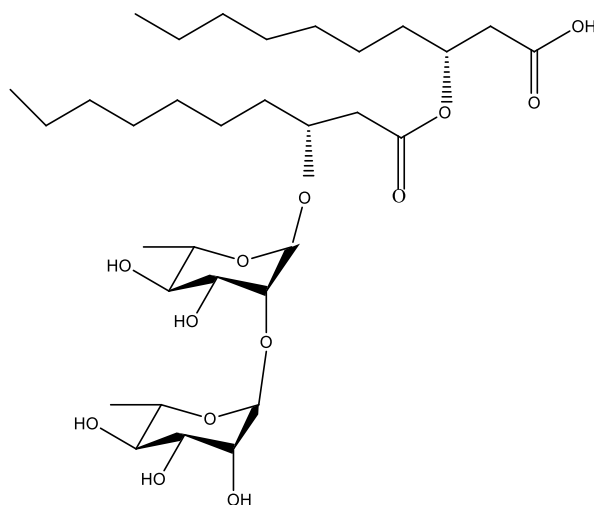
**Figure 24: Fluorescence emission spectra of curcumin conjugated Ag NPs with different concentrations of olic acid.**

# CHAPTER III

## CURCUMIN CONJUGATED SILVER NPs GROWN IN RHAMNOLIPIDS MEDIUM

### 3.1. Introduction

Silver nanoparticles have unique optical, electrical, and thermal properties; therefore, they can be involved in a wide range of applications ranging from photovoltaics to biological and chemical sensors<sup>50</sup>. In synthesizing curcumin conjugated silver nanoparticles in this chapter I used rhamnolipids (a biosurfactant) in water as the growing medium for the curcumin conjugated Ag NPs. Rhamnolipids are glycol-lipids biosurfactants that are produced from *Pseudomonas Aeruginosa* bacteria; and they are classified as mono and di-rhamnolipids<sup>51</sup>. A rhamnolipid is primarily considered as a crystalline acid, and it is composed of  $\beta$ -hydroxy fatty acid that is connected to the carboxyl end of a rhamnose sugar molecule<sup>52</sup>, the structure for dirhamnolipids is shown below:



**dirhamnolipids structure**

There are many species of *Pseudomonas* (P) that are used in the literature to produce rhamnolipids such as: *P. chlororaphis*, *P. plantarii*, *P. putida*, and *P. fluorescens*. Some bacteria can produce mono-rhamnolipids, only while others can produce both. The ratio of mono and di-rhamnolipid can be controlled during the production method. Also there are available enzymes that can convert mono- rhamnolipids into di-rhamnolipids. In the past decades, there were a lot of research on using rhamnolipids in many application as a bio-surfactant, making it one of the most used bio-surfactant materials due to their wide range of applications in various industries because of their “eco-friendly” properties. There are five major applications of rhamnolipids in industry that made them the most used bio-surfactant:

1. Bioremediation and enhanced oil recovery (EOR): Rhamnolipids shows good emulsification properties that extract the crude oil from contaminated soil, especially in petroleum process.
2. Pharmaceuticals and therapeutics: Rhamnolipids are considered as nontoxic and show antimicrobial activities against many kind of bacteria such as: *Bacillus cereus*, *Micrococcus luteus*, *Staphylococcus aureus*, *Listeria mono- cytogen*, etc.
3. Cosmetics: Rhamnolipidis are good effective ingredient on treatment for the skin like that can heal wounds by reducing fibrosis, cure the burn shock and can also be used as wrinkles treatment.
4. Detergents and cleaners: Rhamnolipids are consider as product with a surface active agents so they can be used in detergents compositions, laundry products, shampoos and soaps.

5. Agriculture: Rhamnolipids are used as a soil treatment to improve soil quality, also there is much research that used rhamnolipids as plant pathogen elimination for helping in the absorption of fertilizers and nutrients through roots and as biopesticides.

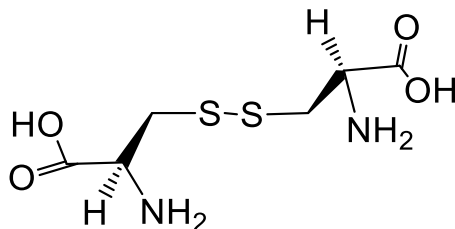
Extraction and use of rhamnolipids in research goes back to 1984, and the first patent for the production of rhamnolipids was by Kaepplian and Guerra-Santos in 1986 for their work on *Pseudomonas aeruginosa* and it was filed by Kaepplian and Guerra-Santos (US 4628030). Then in 1985 Wagner et al. filed a patent (US4814272) for biotechnical production of rhamnolipids from *Pseudomonas* sp<sup>51</sup>.

In the present study we use rhamnolipids as a stabilizer for the preparation of curcumin conjugated Ag NPs. The goal is that it efficiently serves as stabilizer by reducing the Ag NPs aggregation and making uniform morphology. Besides, it is clean, nontoxic (environmental friendly), and economically affordable<sup>51</sup>. Finally, these curcumin conjugated and rhamnolipids stabilized Ag NPs will be tested for optical sensor development. In this Chapter, emphasis will be given for sensing of cystine, albumins (bovine serum albumin and human serum albumin).

### ***3.1.1 Cystine***

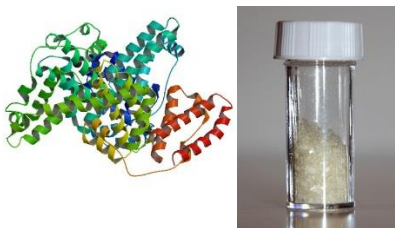
Cysteine is an amino acid that contains a thiol group found in most proteins, and can be found in dairy, eggs, garlic and onions. It can be used as antioxidant in collagen production which is a component in our hair, skin and nails, moreover it can help in the creation of glutathione which is also an important antioxidant. Whereas the cystine formed from combining two cysteine molecules, it is more stable than cysteine and

seldom used in dietary supplement. Also it is a component of hair skin and nails <sup>53</sup>. The structure is given below:



### ***3.1.2 Bovine Serum Albumin (BSA)***

It is a single polypeptide chain consisting of about 583 amino acid residues and no carbohydrates <sup>54</sup> as shown below:

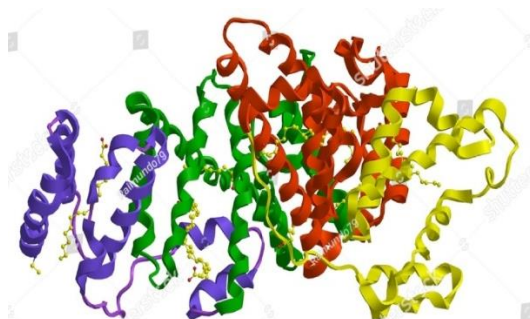


It is also called "Fraction V". BSA is a small, stable, moderately nonreactive protein, so it can be used in many biochemical applications such as ELISAs (Enzyme-Linked Immunosorbent Assay), immunoblots, and as a blocker in immunohistochemistry <sup>55</sup>.

### ***3.1.3 Human Serum Albumin (HSA)***

HSA is an albumin serum found in human blood that is produced from the liver and it is soluble and monomeric, and it forms about half of serum protein. Albumin in general has

many applications like the transport of hormones, fatty acids, and as a pH buffer and many other compounds. Also it maintains oncotic pressure <sup>56</sup>.



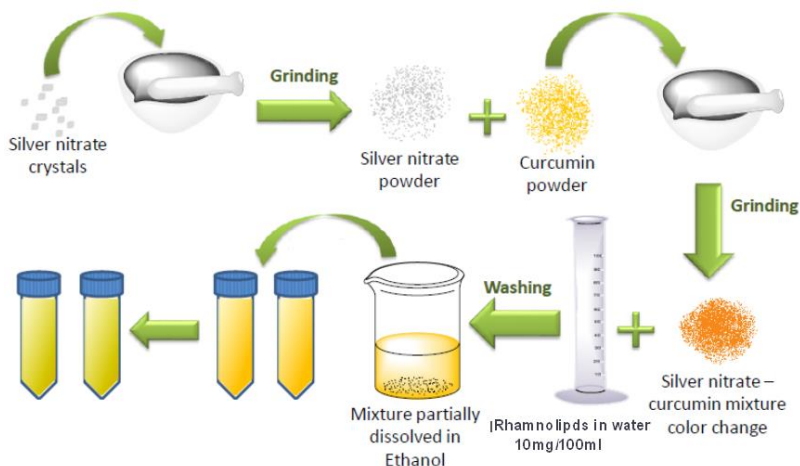
### **3.2. Materials**

Curcumin, silver nitrate obtained from Sigma–Aldrich were directly used without further purification. Rhamnolipids from Sigma-Aldrich were prepared in double distilled water (DDW). For rhamnolipids stock solution, 10 mg of the rhamnolipid was dissolved in 100 mL of DDW. For sensing Albumin Serum from bovine blood and human blood, 66 mg of each of them was dissolved in 2 mL DDW to prepare the stock solution. For cystine sensing, 45 mg of cystine was dissolved in 5 mL NaOH solution to prepare the stock solution.

### **3.3. Instrumentation**

As described in previous chapter.

### 3.4. Synthesis of curcumin conjugated Ag NPs



A stock of rhamnolipid solution was prepared by dissolving 10 mg of the rhamnolipid in 100 mL of DDW. Then 169.7 mg of crystals silver nitrate (1.0 mol) and 184.19mg (0.5 mol) of curcumin were mixed and grinded in a marble mortar using a pestle until the crystals were crushed and turned into powder and the color changed from yellow to dark orange approximately after 30 minutes. The powder mixture was then partially dissolved in 100 mL of rhamnolipid water solution, after that the solution mixture was transferred into two 50 mL falcon tubes, the total volume of the solution mixture was approximately 95 mL. The growth of the nanoparticles continued in rhamnolipids water solution for 1, 2, 4, 8, 16 hours and 1, 2, 3, 5, and 7 days at 60°C. Then after the growth time ended, we centrifuged the samples for 20 minutes at 4000 rpm at 20°C, to remove all the unbounded or unreacted curcumin from the solutions by using acetone and centrifuged it, then we discarded the solution (yellow solution). We repeated the washing part several times (around 5 times) until the supernatant was clear of all the curcumin. After finishing the washing part, we got rid of all the acetone, and added 10 mL of water in 50 mL tubes, and stored it for later study.

### 3.5. Results and discussion

The curcumin conjugate Ag NPs were prepared in the solid state by the participation of silver nitrate and curcumin as starting materials and using the curcumin as a reducing agent to reduce  $\text{Ag}^+$  in silver nitrate to  $\text{Ag}^0$  the metallic form. Curcumin and silver nitrate were mixed in their solid state at 60 °C for ten different growing times 1, 2, 4, 8, 16 hours and 1, 2, 3, 5, 7 days. After grinding the starting material in the solid state we noticed a change in the color from bright yellow to orange. Then we delivered the solid mixture in the rhamnolipid-water solution mixture to grow Ag nanoparticles. After the period of time ended, we centrifuged the sample for 20 minutes and washed it by acetone until we got rid of all the yellow color and had a transparent solution. After having the transparent solution, we discarded all the acetone and added double distilled water to store it and use it in different studies. Some of the Ag NPs must also be lost to the solution during washing. For SEM, UV-visible and fluorescence spectroscopic studies we took 1 mL from the sample and added 3 mL DDW in a small vial, whereas for sensing studies we took directly from the stock sample tube with no further dilution.

### 3.6. Characterization

#### *X-ray diffraction analysis (XRD)*

The particles were collected in the same way as in Chapter II, and also we obtained similar results. The XRD pattern of curcumin-conjugated Ag NPs is shown in Figure 25. The sharp Bragg reflection in the XRD spectrum indicates the presence of organic content associated with Ag NPs. All the major peaks in XRD can be indexed for the face centered cubic structure of Ag NPs. The different peaks originated from the (1 1 1), (2 0



0), (2 2 0), and (3 1 1) planes of Ag NPs perfectly match with the JCPDS card number 4-0783<sup>41</sup>. A major peak at lower  $2\theta$  value might be due to the organic content of curcumin. The XRD pattern further reveals that curcumin conjugated silver nanoparticles are crystalline in nature. The average diameter of silver nanoparticles can be estimated from the (111) diffraction peak using Scherrer's equation as  $L = 0.91 \lambda / (\beta \cos \alpha)$  where  $L$  is the mean crystallite size,  $\lambda$  is the wavelength of incident rays (1.5405 Å),  $\beta$  is the full width at half maximum (FWHM) of the highest intensity peak in radians, and  $\alpha$  is the center angle of the peak in radian<sup>37</sup>. The mean crystallite size for Ag NPs was determined to be 8.47 nm by using this formula, and the values were lower than what was found in SEM images.

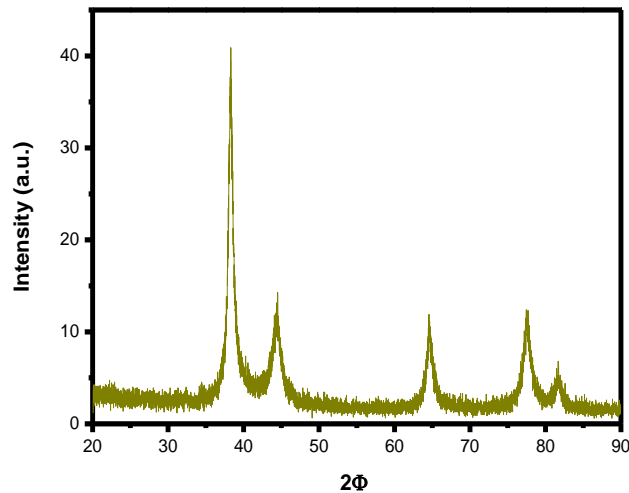
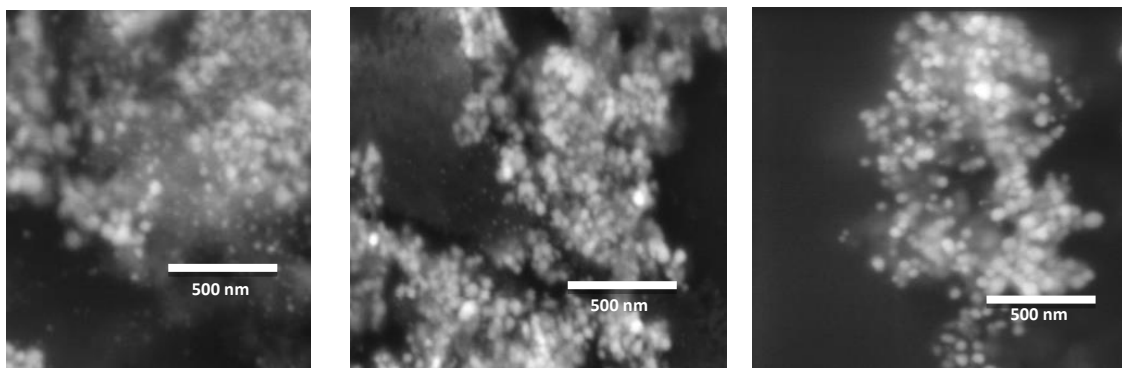


**Figure 25: XRD pattern of curcumin conjugated and rhamnolipids stabilized Ag NPs prepared after 2 days of growth time at 60°C.**

### *Scanning electron microscopy (SEM)*

The SEM images recorded mostly in 500 nm resolution, show variation in the size of Ag NPs with ten different growth times at the four different temperatures. Figure 26 shows how the particles became bigger with different times, the 1 hour growth time sample shows very small particles size that we couldn't see in SEM, and the same case was with 2,4,8,16 hours growth time samples. However, in one day growth time sample the particles ranged between 10-30 nm with spherical shapes, two days growth time sample also shows bigger size between 20-40 nm with spherical shapes. The 3 and 5 days growth time samples the particles size ranged between 20-50 nm diameter with spherical shapes, but with 7 days growth time sample we found a diversity in the shapes of the curcumin conjugated Ag NPs where rods shape started to appear, the radius of the spherical particles diameter ranged between 40-60 nm. Many of the SEM pictures show imperfection, some blurriness or unclear images due to the presence of unreacted curcumin in the sample on the conjugated curcumin Ag NPs during the sample preparation we noticed there was a change in sample color from light yellow in the one hour growth time sample to darker yellow or orange in the seven days sample.



1hour

2hours

4hours

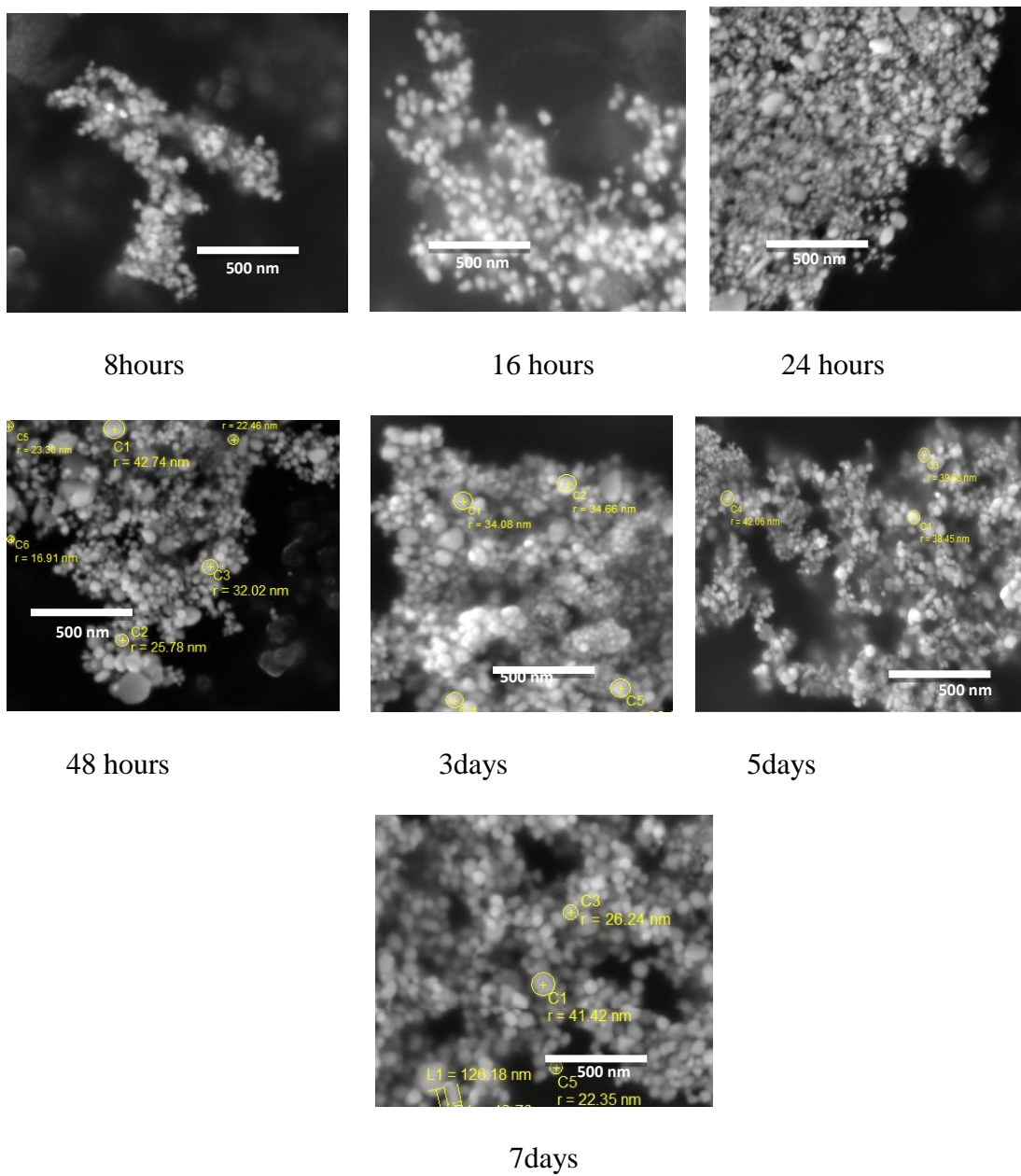


**Figure 26: SEM images of curcumin conjugated and rhamnolipids stabilized Ag NPs in different growth time intervals at 60°C.**

### 3.7. Spectroscopic measurement

#### *UV-VIS spectroscopy*

The UV-visible spectra recorded at ten different growth times are given in Figure 27A, we noticed different peaks and intensities for the different growth times due to the different sizes and shapes. Curcumin strongly absorbs at around 266 nm for  $S_1 - S_2$  transition and at around 425 nm for  $S_0 - S_1$  transition in aqueous medium <sup>43</sup>. However, the mixture of curcumin and  $AgNO_3$  that was used to prepare Ag NPs shows absorbance peaks around 400 nm as the time increased absorbance changes. The sharp peak observed at 250 nm is due to  $Ag^+$  bounded to curcumin <sup>44</sup>. The curcumin has the ability to chelate on the cation metals like  $Zn^{+2}$  and  $Cu^{+2}$  where those cation will bind to C=O group of the  $\beta$ -diketone moiety on curcumin <sup>45</sup>. The absorbance peaks for Ag NPs appear because of the elastic scattering phenomenon, known as Surface Plasmon resonance (SPR).

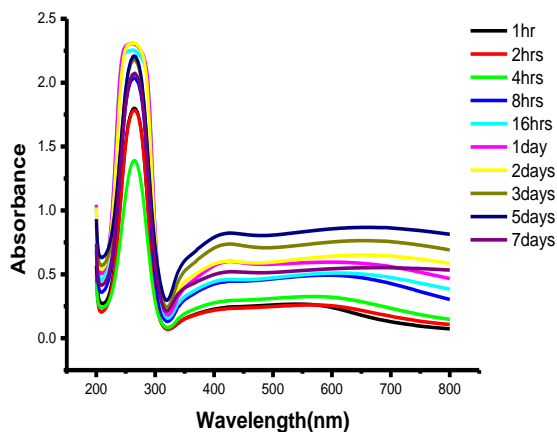


**Figure 27: UV-VIS spectra of curcumin conjugated and rhamnolipids stabilized Ag NPs prepared in different growth time intervals at 60°C.**

### Fluorescence spectroscopy

The fluorescence spectra of curcumin conjugated silver nanoparticles were recorded with an excitation wavelength 425 nm, and the fluorescence emission spectra were recorded in from 440–600 nm, similar to reported for curcumin in different solvent environment <sup>47</sup>. In a pure solution of curcumin in polar solvent like water a broad peak at 550 nm appears in the emission spectra <sup>9,44</sup>, whereas in the present sample of curcumin conjugated and rhamnolipids stabilized Ag NPs only one strong peak appeared at ~ 490 nm as maximum in water as shown in Figure 28A. The fluorescence intensity increased with growth time, more growth time (with bigger particles) gave higher fluorescence intensity as depicted in Figure 28B.

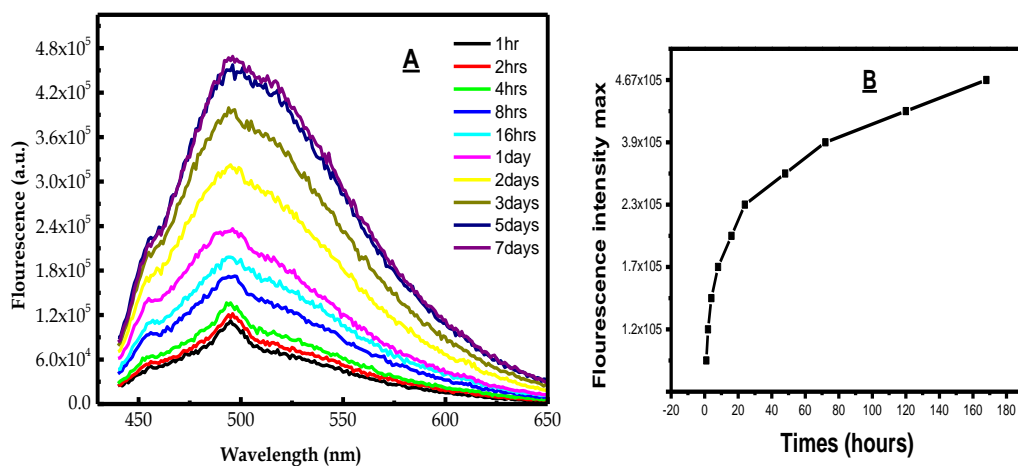


**Figure 28:** (A) Fluorescence emission spectra of curcumin conjugated and rhamnolipids stabilized Ag NPs in different growth time intervals at 425 nm excitation wavelength, (B) Fluorescence intensity vs growth times in hours for curcumin conjugated and rhamnolipids stabilized Ag NPs in different growth time intervals.

The Resonance Rayleigh Scattering spectra as shown in Figure 29A were measured by applying synchronous fluorescence spectra by keeping the wavelength interval  $\Delta\lambda$  at 0 nm the difference between emission and excitation 0. The Resonance Rayleigh Scattering spectrum of curcumin conjugated Ag NPs at 60 °C for ten different growth times showed four bands each one has different SFS intensity and wavelength. First two bands are the excitation bands which is similar to what we have in Figure 8, and the other two are around the emission band regions of curcumin conjugated Ag NPs particles. As expected, bigger particles have higher SFS intensity and it shifts the scattering peak to longer wavelength region. It reached a maximum at 600 nm and a higher SFS intensity at  $4.2 \times 10^8$  for the 7, 5, 3 days growth samples, which have a bigger particle size. Figure 29B shows that the SFS intensity reaches a steady state for longer growth time, (no further increase in SFS intensity for 3, 5, 7 days growth samples), which is evident because these samples contain particles size ranging from 40 nm-60 nm.

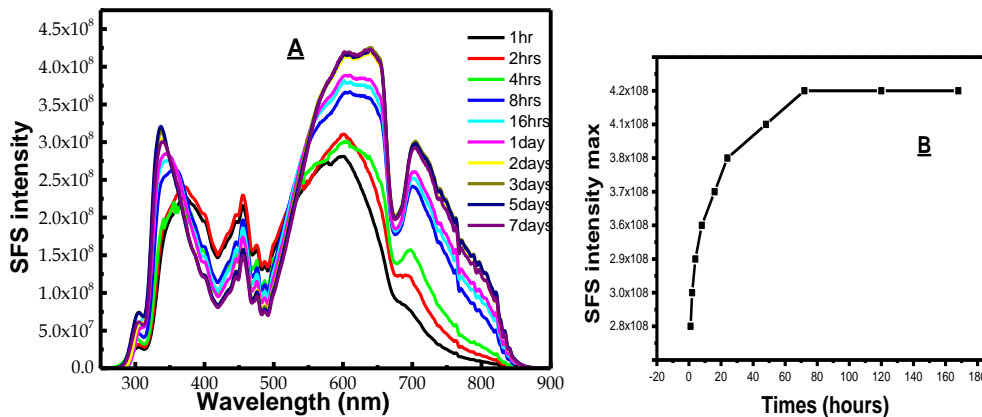


**Figure 29: (A) Synchronous fluorescence spectra of curcumin conjugated and rhamnolipids stabilized Ag NPs in different growth time intervals at 425 nm excitation wavelength; (B) Synchronous fluorescence intensity vs (growth) times in hours for curcumin conjugated and rhamnolipids stabilized Ag NPs in different growth time intervals.**

### **3.8. Sensing studies**

Determination of cystine, bovine blood serum albumin (BSA) and human blood serum albumin (HAS) are important in molecular biology, therefore we used our curcumin conjugated silver nanoparticles in sensing those three compounds, by doing fluorescence emission spectroscopic measurement, and determining the association constant  $K$  and  $n$  the number of binding sites.

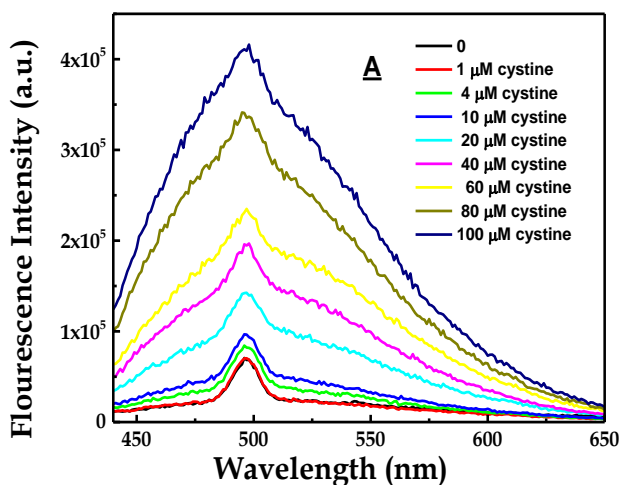
#### **Cystine**

Fluorescence spectroscopic measurement of curcumin conjugated silver nanoparticles was carried out in various concentrations of cystine from  $1\mu\text{M}$  to  $100\mu\text{M}$  range and by fixing the concentration of curcumin conjugated and rhamnolipids stabilized Ag NPs, which was  $0.5\text{ mL}$ . We prepared the cystine stocked solution by dissolving  $181\text{ mg}$  of cystine in  $5\text{ mL}$  of alkaline medium (NaOH+DDW) ( $258\text{mg}$  of NaOH in  $30\text{ml}$  DDW). Upon binding of cystine, the fluorescence of curcumin conjugated and rhamnolipids stabilized silver nanoparticles enhanced remarkably as shown in Figure 30A. The spectral position (emission maximum) stayed in the same region without any change. However, with increase concentration of cystine the fluorescence intensity increased. Higher concentrations gave higher fluorescence intensities, because it forms a complexation with curcumin conjugated silver nanoparticles. The addition of cystine concentrations will further stabilize the excited state of curcumin conjugated silver nanoparticles. The calibration curve as depicted in Figure 30B showed a regular change in fluorescence intensity vs. cystine concentration and could be easily applied for quantifying unknown

cystine samples. For further understanding of the affinity of cystine towards curcumin conjugated Ag NPs, the association constant and number of binding sites were estimated. For molecules that bind independently to a set of equivalent sites in a macromolecule, the equilibrium between unbound and bound molecules can be given as (see Appendix 3) <sup>57</sup>:

$$\log \frac{F-F_0}{F_0} = \log K + n \log[\text{cystine}]$$

K are the binding constant, n is the number of binding sites, F and F<sub>0</sub> are the fluorescence intensity of curcumin conjugated Ag NPs bound and unbound to cystine respectively. The plot of log (F – F<sub>0</sub>)/F<sub>0</sub> versus log [cystine] is illustrated in Figure 30C and found to be linear. The calculated values for n= 1.01 and K= 5.4 x10<sup>4</sup> M<sup>-1</sup> which suggest that there is strong binding affinity between cystine and Ag NPs. The present n value could be due to binding between cystine molecules and curcumin, which suggest a 1:1 binding ratio.





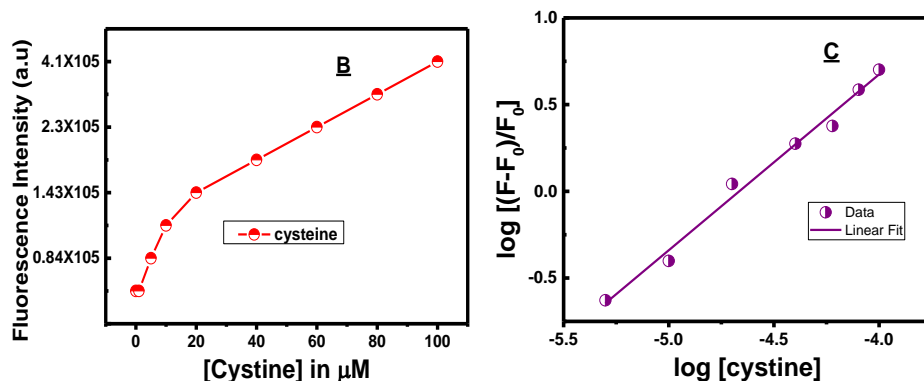


**Figure 30: (A) Fluorescence emission spectra of curcumin conjugated and rhamnolipids stabilized Ag NPs in the presence of various concentration of cystine; (B) Calibration curve for estimation of cystine by monitoring fluorescence intensity of curcumin conjugated Ag NPs; (C) Plot of cystine concentration vs.  $(F - F_0)/F_0$  while determining association constant of cystine with curcumin conjugated and rhamnolipids stabilized Ag NPs.**

### **Bovine Serum Albumin (BSA)**

For estimation of BSA, we took 66 mg of BSA dissolved in 2 mL DDW then taking different amounts of this solution, we prepared BSA concentration in the range between 0 and 100  $\mu\text{M}$ . When the BSA binds to curcumin conjugated and rhamnolipids stabilized Ag NPs the fluorescence spectra enhanced remarkably as shown in Figure 31A, however, the wavelength maximum and spectral position stayed the same. With increasing concentration of BSA the fluorescence intensity increased. Higher concentrations gave higher fluorescence intensities, because it forms a complexation with curcumin conjugated silver nanoparticles. The calibration curve as depicted in Figure 31B showed a regular change in fluorescence intensity vs. BSA concentration, and we can also apply it to quantify unknown BSA samples. We measured the affinity of BSA towards curcumin conjugated Ag NPs, the association constant  $k$  and number of binding sites  $n$

were estimated applying the equation as described above. The plot of  $\log (F - F_0)/F_0$  versus  $\log [BSA]$  is illustrated in Figure 31C and found to be linear. The calculated values for  $n = 0.2$  the slope and  $K = 13 \text{ M}^{-1}$  which suggest that there is relatively a weak binding affinity between BSA and Ag NPs and one BSA is associated with about 5 Ag NPs.

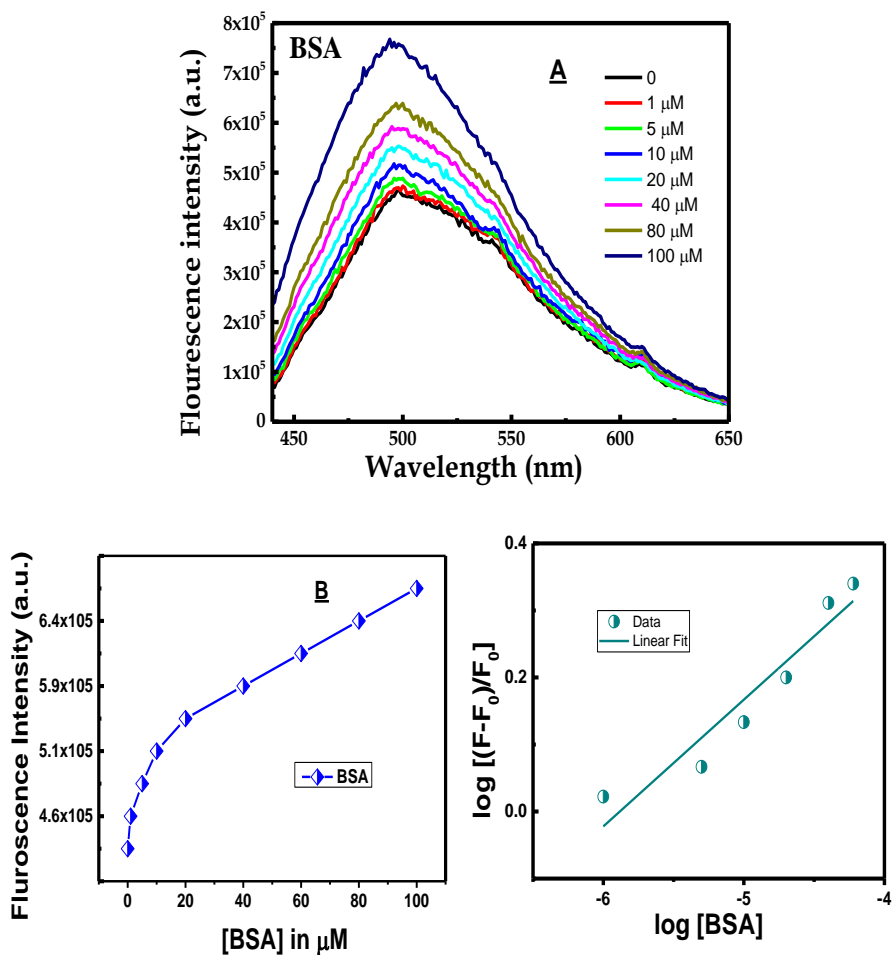


**Figure 31: (A) Fluorescence emission spectra of curcumin conjugated and rhamnolipids stabilized Ag NPs in the presence of various concentration of BSA; (B) Calibration curve for estimation of BSA by monitoring fluorescence intensity of curcumin conjugated Ag NPs; (C) Plot of BSA concentration vs.  $(F - F_0)/F_0$  while determining association constant of BSA with curcumin conjugated Ag NPs.**

## **Human Serum Albumin (HSA)**

Finally, we measured the emission of HSA with curcumin conjugated Ag NPs, by dissolving 66 mg of HSA in 2 mL DDW. The concentration of HSA studied in this case was between 0 and 100 $\mu$ M. When the HSA binds to curcumin conjugated Ag NPs, it enhances the fluorescence spectra as shown in Figure 32A, the spectral wavelength and position stayed the same with all the different concentrations. However, with increasing concentration of HSA fluorescence intensity increased. Higher concentrations gave us higher fluorescence intensities, because it forms a complexation with curcumin conjugated silver nanoparticles. The calibration curve as depicted in Figure 32B showed a regular change in fluorescence intensity vs. HSA concentration, and it's also can be applied for quantifying unknown HSA samples. We measured the affinity of HSA towards curcumin conjugated Ag NPs, the association constant  $k$  and number of binding sites  $n$  as per the equation explained earlier. The plot of  $\log (F - F_0)/F_0$  versus  $\log [HSA]$  is depicted in Figure 32C and found to be linear. The calculated values for  $n= 0.6$  the slope and  $K= 213.8 \text{ M}^{-1}$ . This suggests that there is relatively higher binding affinity for HSA compared to BSA, but it is still less than cystine.

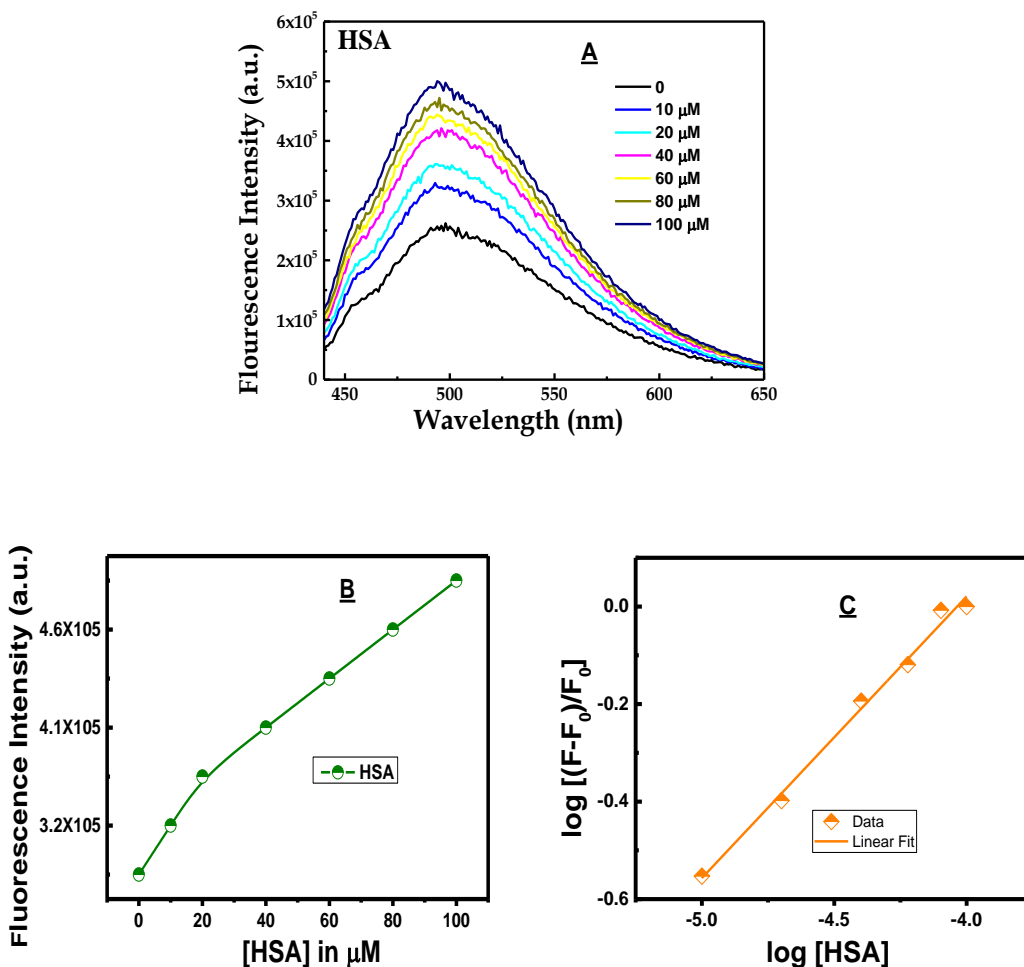


**Figure 32: (A) Fluorescence emission spectra of curcumin conjugated and rhamnolipid stabilized Ag NPs in the presence of various concentration of HSA; (B) Calibration curve for estimation of HSA by monitoring fluorescence intensity of curcumin conjugated Ag NPs; (C) Plot of HSA concentration vs.  $(F - F_0)/F_0$  while determining association constant of HSA with curcumin conjugated Ag NPs**

## CHAPTER IV

### CONCLUSION

Silver nanoparticles have fascinated the scientists from different fields in the last decades because of their small size, they have a large surface area to volume ratio, also the presence of surface Plasmon resonance, which gives them different chemical and physical properties like mechanical properties, biological, catalytic activity, thermal and electrical conductivity, and optical absorption. The size of Ag NPs ranging from 1-100 nm, all of these properties will be different with their bigger size counterparts. Therefore, nanoparticles have size and shape dependent properties, so different size and shapes can give different properties also different applications ranging from biosensing and catalysts to optics. So we can synthesize different shapes and sizes of nanoparticles by controlling the synthetic process. In the present days scientists are synthesizing Ag NPs with different sizes and shapes by using the different synthetic process like using reducing agents such as  $\text{NaBH}_4$ , or laser irradiation technique, etc. Those different Ag NPs can be applied in many different applications. Many of the synthetic processes can pollute the environment by decomposing toxic materials, so researchers want to reduce, treat and prevent this pollution by using non-toxic material eco-friendly in synthesizing new chemical materials so they invented “green chemistry” term. In my work, we synthesized Ag NPs by using a green synthetic route where we used non-toxic materials like curcumin as reducing agents to reduce  $\text{Ag}^+$  to  $\text{Ag}^0$  metallic form, silver nitrate and an organic medium. Here in my thesis, I used ethanol as the organic medium in the first part and rhamnolipids in water (10 mg/100 mL) in the second part.

The curcumin conjugate Ag NPs were prepared through a solid state chemistry by the participation of silver nitrate (1mole) and curcumin (0.5) as a starting material and using the curcumin as a reducing agent to reduce  $\text{Ag}^+$  in silver nitrate to  $\text{Ag}^0$  the metallic form, the color of the solid materials changed from yellow to orange. I preserved the orange powder in an organic medium 100 ml of ethanol and rhamnolipids in water (10g/100ml).

I used four different temperatures 4 °C, room temperature ~20°C, 40°C and 60°C in synthesizing curcumin conjugated Ag NPs and I preserve my sample in ethanol for ten different growth times 1,2,4,8,16 hours and 2,3,5,7 days. I used ethanol as a medium to grow the curcumin conjugated Ag NPs, and in washing the sample to get rid of all unreacted curcumin, by centrifuging the samples for 20 minutes at 4000 speed until the color of the supernatant changes from yellow to transparent. Then we throw the ethanol and add water to the residue and used in the application. By reading the samples with SEM we noticed that with higher temperature and more time the particles size became bigger and more variety in shapes, for example in 4°C we have only spherical shapes but in 60°C we have spherical, rods, and most of them are hexagonal, also in 60°C in 5 and 7 days the size of the particle exceeded the nano scale reached the micro scale. In UV-VIS spectroscopy we noticed that curcumin conjugated Ag NPs shows absorbance peaks around 440-450 nm in all temperatures and as the time increased in the same temperature, the peaks shifted to 500 nm with bigger particles. Sharp peaks were noticed at around 250 nm this is due to  $\text{Ag}^+$  bounded to C=O group of the  $\beta$ -diketone moiety on curcumin because curcumin has the ability to chelate on the cation metals (M-L). In fluorescence spectroscopy, we found that curcumin conjugated Ag NPs have emission spectra at ~ 490 nm as a maximum for all the temperatures at ten different times only the fluorescence

intensities changed, higher intensity more time means bigger particles. Curcumin conjugated Ag NPs prepared at the different temperatures at ten different times can be an excellent catalyst for the reduction of 4-nitrophenol to 4-aminophenol, wherein the reduction happened on the surface of Curcumin conjugated Ag NPs. However, from the calculation of the  $t_{1/2}$ , we found that Ag NPs that prepared at 20°C gives the lowest  $t_{1/2}$  higher rate constant from the equation:

$$t_{1/2}=0.693/k.$$

Curcumin conjugated Ag NPs can be used as a bio sensing for detecting fatty acids like 6-O-palmitoyl-L-ascorbic acid. Whenever 6-O-palmitoyl-L-ascorbic acid interacts with Curcumin conjugated Ag NPs and forming a complex, the intensity of RRS/fluorescence signal will greatly increase with the increase in the 6-O-palmitoyl-L-ascorbic acid concentration, and the wavelength stayed fixed. I prepared my curcumin conjugated Ag NPs at 60°C a for ten different times 1,2,4,8,16 hours and 2,3,5,7 days, and I preserve them in Rhamnolipids with water (10mg/100ml). I used acetone in washing the samples to get rid of all the unreacted curcumin, by centrifuging the samples for 20 minutes at 4000 speed until the color of the supernatant changes from yellow to transparent. Then we throw the acetone and add water to the residue.

By reading the samples with SEM we noticed that with more time the particles size become bigger. In UV-VIS spectroscopy we noticed that curcumin conjugated Ag NPs shows absorbance peaks around ~400nm at all times, other peaks were noticed at ~250nm this is due to Ag<sup>+</sup> bounded to C=O group of the  $\beta$ -diketone moiety on curcumin because curcumin has the ability to chelate on the cation metals (M-L), only the

absorbance changes with time. In fluorescence spectroscopy, we found that curcumin conjugated Ag NPs have an emission spectra at ~ 490 nm as a maximum for all ten different times only the fluorescence intensities changed higher intensity more time means bigger particles. Curcumin conjugated Ag NPs can be used as a bio sensing for detecting some of the amino acids like L(-)Cystin, and proteins like BSA and HAS. Where they interact with Curcumin conjugated Ag NPs and forming a complex the intensity of RRS/fluorescence signal will greatly increase by increasing the concentrations where the wavelength stayed fixed.

Finally, the differences between the Curcumin conjugated Ag NPs that preserved in ethanol and Rhamnolipids in water is in the particles size at 60°C were the particle in ethanol noticed to be bigger than in Rhamnolipids.



## APPENDIX 1

### First rate constant derivative

$$\mathbf{rate = k[A]}$$

$$-\frac{d[A]}{dt} = k[A]$$

$$\int_{[A]_0}^{[A]} \frac{d[A]}{[A]} = - \int_{t_0}^t k dt$$

$$\int_{[A]_0}^{[A]} \frac{1}{[A]} d[A] = - \int_{t_0}^t k dt$$

*Upon integrating:*

$$\ln [A] - \ln [A]_0 = -kt$$

$$\ln \left( \frac{[A]}{[A]_0} \right) = -kt$$

❖ **For half-lives of first order reactions:**

$$[A] = \frac{1}{2} [A]_0$$

After a period of one half-life,  $t = t_{1/2}$  and we can write:

$$\frac{[A]_{1/2}}{[A]_0} = \frac{1}{2} = e^{-kt_{1/2}}$$

$$\ln 0.5 = -kt$$

$$t_{1/2} = \frac{\ln 2}{k} \approx \frac{0.693}{k}$$

## APPENDIX 2

### Relation between particle size and surface to volume ratio

$\frac{S}{V}$  is greater for smaller particles

$$\text{Since } \frac{S}{V} = \frac{4\pi r^2}{\frac{4}{3}\pi r^3} = \frac{3}{r}$$

For example, if we have 3 balls, one small, one medium, and one large, the smallest ball has smaller internal content (volume) compared to its outside surface area. Therefore it has a big surface area compared to its volume, so a high surface area to volume ratio. In the medium ball, compared to the smaller ball, the surface area has not increased hugely, but the internal content (volume) will be much greater, this means that surface area to volume ratio is reduced. In the biggest ball the surface area covering the ball has not increased significantly but the internal content has increased greatly bringing the surface area to volume ratio down (making it smaller) because the internal volume is far greater than the outside surface area.

### APPENDIX 3

#### Derivation for Estimating Binding Constant



$$K = \frac{[C]}{[A][B]^n}$$

$$\log K = \log \frac{[C]}{[A]} - n \log [B]$$

$$\log K = \log \frac{F}{F_0 - F} - n \log [B]$$

$$\log \frac{F}{F_0 - F} = \log K + n \log [B]$$

In the present case fluorescence intensity increases of Ag NPs after binding, so for unbound form it is  $F_0$ , and for bound form  $F - F_0$ , thus

in terms of fluorescence change this can be rewritten as:

$$\log \frac{F_0 - F}{F_0} = \log K + n \log [B]$$

## REFERENCES

1. Sheldon, R. A.; Arends, I. W.; Hanefeld, U., Introduction: Green chemistry and catalysis. *Green Chemistry and Catalysis* **2007**, 1-47.
2. El Khoury, E. D.; Patra, D., Ionic liquid expedites partition of curcumin into solid gel phase but discourages partition into liquid crystalline phase of 1, 2-dimyristoyl-sn-glycero-3-phosphocholine liposomes. *The Journal of Physical Chemistry B* **2013**, *117* (33), 9699-9708.
3. Fahlman, B. D., What is Materials Chemistry? In *Materials chemistry*, Springer: 2011; pp 1-12.
4. Iravani, S., Green synthesis of metal nanoparticles using plants. *Green Chemistry* **2011**, *13* (10), 2638-2650.
5. Mody, V. V.; Siwale, R.; Singh, A.; Mody, H. R., Introduction to metallic nanoparticles. *Journal of Pharmacy and Bioallied Sciences* **2010**, *2* (4), 282.
6. Kneipp, K.; Kneipp, H.; Itzkan, I.; Dasari, R. R.; Feld, M. S., Ultrasensitive chemical analysis by Raman spectroscopy. *Chemical reviews* **1999**, *99* (10), 2957-2976.
7. Evanoff, D. D.; Chumanov, G., Synthesis and optical properties of silver nanoparticles and arrays. *ChemPhysChem* **2005**, *6* (7), 1221-1231.
8. <Principles of Fluorescence Spectroscopy.pdf>
9. Patra, D.; Mishra, A., Recent developments in multi-component synchronous fluorescence scan analysis. *TrAC Trends in Analytical Chemistry* **2002**, *21* (12), 787-798.
10. Prakash, S.; Soni, N., Factors affecting the geometry of silver nanoparticles synthesis in *Chrysosporium tropicum* and *Fusarium oxysporum*. *American journal of nanotechnology* **2011**, *2* (1), 112-121.
11. Biswas, P. K.; Dey, S., EFFECTS AND APPLICATIONS OF SILVER NANOPARTICLES IN DIFFERENT FIELDS. **2015**.
12. Kotthaus, S.; Gunther, B. H.; Hang, R.; Schafer, H., Study of isotropically conductive bondings filled with aggregates of nano-sited Ag-particles. *IEEE Transactions on Components, Packaging, and Manufacturing Technology: Part A* **1997**, *20* (1), 15-20.
13. Cao, G., *Nanostructures and nanomaterials: synthesis, properties and applications*. World Scientific: 2004.
14. Zhang, W.-z.; Wang, G., Research and development for antibacterial materials of silver nanoparticle. *New Chem Mater* **2003**, *31* (2), 42-44.
15. Klaus-Joerger, T.; Joerger, R.; Olsson, E.; Granqvist, C.-G., Bacteria as workers in the living factory: metal-accumulating bacteria and their potential for materials science. *TRENDS in Biotechnology* **2001**, *19* (1), 15-20.
16. Krishnaraj, C.; Jagan, E.; Rajasekar, S.; Selvakumar, P.; Kalaichelvan, P.; Mohan, N., Synthesis of silver nanoparticles using *Acalypha indica* leaf extracts and its antibacterial activity against water borne pathogens. *Colloids and Surfaces B: Biointerfaces* **2010**, *76* (1), 50-56.
17. Mansur, H. S.; Grieser, F.; Marychurch, M. S.; Biggs, S.; Urquhart, R. S.; Furlong, D. N., Photoelectrochemical properties of 'Q-state' CdS particles in arachidic acid Langmuir-Blodgett films. *Journal of the Chemical Society, Faraday Transactions* **1995**, *91* (4), 665-672.
18. Cho, K.-H.; Park, J.-E.; Osaka, T.; Park, S.-G., The study of antimicrobial activity and preservative effects of nanosilver ingredient. *Electrochimica Acta* **2005**, *51* (5), 956-960.

19. Durán, N.; Marcato, P. D.; De Souza, G. I.; Alves, O. L.; Esposito, E., Antibacterial effect of silver nanoparticles produced by fungal process on textile fabrics and their effluent treatment. *Journal of biomedical nanotechnology* **2007**, *3* (2), 203-208.
20. Puišo, J.; Jonkuvienė, D.; Mačionienė, I.; Šalomskienė, J.; Jasutienė, I.; Kondrotas, R., Biosynthesis of silver nanoparticles using lingonberry and cranberry juices and their antimicrobial activity. *Colloids and Surfaces B: Biointerfaces* **2014**, *121*, 214-221.
21. Abid, J.-P.; Wark, A.; Brevet, P.-F.; Girault, H., Preparation of silver nanoparticles in solution from a silver salt by laser irradiation. *Chemical Communications* **2002**, (7), 792-793.
22. Itakura, T.; Torigoe, K.; Esumi, K., Preparation and characterization of ultrafine metal particles in ethanol by UV irradiation using a photoinitiator. *Langmuir* **1995**, *11* (10), 4129-4134.
23. Pol, V. G.; Srivastava, D.; Palchik, O.; Palchik, V.; Slifkin, M.; Weiss, A.; Gedanken, A., Sonochemical deposition of silver nanoparticles on silica spheres. *Langmuir* **2002**, *18* (8), 3352-3357.
24. Stiger, R.; Gorer, S.; Craft, B.; Penner, R., Investigations of electrochemical silver nanocrystal growth on hydrogen-terminated silicon (100). *Langmuir* **1999**, *15* (3), 790-798.
25. Harfenist, S. A.; Wang, Z.; Alvarez, M. M.; Vezmar, I.; Whetten, R. L., Highly oriented molecular Ag nanocrystal arrays. *The Journal of Physical Chemistry* **1996**, *100* (33), 13904-13910.
26. El Khoury, E.; Abiad, M.; Kassaify, Z. G.; Patra, D., Green synthesis of curcumin conjugated nanosilver for the applications in nucleic acid sensing and anti-bacterial activity. *Colloids and Surfaces B: Biointerfaces* **2015**, *127*, 274-280.
27. Wiley, B.; Sun, Y.; Mayers, B.; Xia, Y., Shape-controlled synthesis of metal nanostructures: the case of silver. *Chemistry-A European Journal* **2005**, *11* (2), 454-463.
28. Evanoff, D. D.; Chumanov, G., Size-controlled synthesis of nanoparticles. 2. Measurement of extinction, scattering, and absorption cross sections. *The Journal of Physical Chemistry B* **2004**, *108* (37), 13957-13962.
29. Nurani, S. J.; Saha, C. K.; Arifur Rahman Khan, M., *Silver Nanoparticles Synthesis, Properties, Applications and Future Perspectives: A Short Review*. 2015; Vol. 10, p 117-126.
30. Ghosh, S.; Harke, A.; Chacko, M.; Gurav, S.; Joshi, K., Gloriosa superba Mediated Synthesis of Silver and Gold Nanoparticles for Anticancer Applications. *J Nanomed Nanotechnol* **2016**, *7* (390), 2.
31. Mukunthan, K.; Balaji, S., Cashew apple juice (*Anacardium occidentale* L.) speeds up the synthesis of silver nanoparticles. *International Journal of Green Nanotechnology* **2012**, *4* (2), 71-79.
32. Gavade, S. M.; Nikam, G.; Sabale, S.; Tamhankar, B., Green synthesis of fluorescent silver nanoparticles using Acacia nilotica gum extract for kinetic studies of 4-nitrophenol reduction. *Materials Today: Proceedings* **2016**, *3* (10), 4109-4114.
33. Priyadarsini, K. I., The chemistry of curcumin: from extraction to therapeutic agent. *Molecules* **2014**, *19* (12), 20091-20112.
34. Pabon, H., A synthesis of curcumin and related compounds. *Recueil des Travaux Chimiques des Pays-Bas* **1964**, *83* (4), 379-386.
35. Kim, J.-S., Reduction of silver nitrate in ethanol by poly (N-vinylpyrrolidone). *Journal of Industrial and Engineering Chemistry* **2007**, *13* (4), 566-570.
36. Polte, J., Fundamental growth principles of colloidal metal nanoparticles—a new perspective. *CrystEngComm* **2015**, *17* (36), 6809-6830.
37. Hacisevki, A., An overview of ascorbic acid biochemistry. *J Fac Pharm Ankara* **2009**, *38*, 233-255.
38. De Ritter, E.; Cohen, N.; Rubin, S. H., Physiological availability of dehydro-L-ascorbic acid and palmitoyl-L-ascorbic acid. *Science (Washington)* **1951**, *113*, 628-631.

39. Thomas, A.; Matthäus, B.; Fiebig, H. J., Fats and fatty oils. *Ullmann's Encyclopedia of Industrial Chemistry* **2000**.
40. McCrudden, F. H., *Uric Acid*. BiblioBazaar, LLC: 2008.
41. Park, H.-H.; Zhang, X.; Choi, Y.-J.; Park, H.-H.; Hill, R. H., Synthesis of Ag Nanostructures by Photochemical Reduction Using Citrate-Capped Pt Seeds. *Journal of Nanomaterials* **2011**, *2011*, 1-7.
42. Liu J.; Song S.; Wang F.; Song Y.; Mater J., *2*, 17477–17488
43. El Kurdi, R.; Patra, D., The role of OH<sup>-</sup> in the formation of highly selective gold nanowires at extreme pH: multi-fold enhancement in the rate of the catalytic reduction reaction by gold nanowires. *Physical chemistry chemical physics : PCCP* **2017**, *19* (7), 5077-5090.
44. Kundu, S.; Nithiyantham, U., In situ formation of curcumin stabilized shape-selective Ag nanostructures in aqueous solution and their pronounced SERS activity. *RSC Advances* **2013**, *3* (47), 25278-25290.
45. Zhao, X.-Z.; Jiang, T.; Wang, L.; Yang, H.; Zhang, S.; Zhou, P., Interaction of curcumin with Zn (II) and Cu (II) ions based on experiment and theoretical calculation. *Journal of Molecular Structure* **2010**, *984* (1), 316-325.
46. <HL08 effect of solvent on the excited-state photophysical properties of curcumin.pdf>.
47. Patra, D.; Barakat, C., Synchronous fluorescence spectroscopic study of solvatochromic curcumin dye. *Spectrochimica Acta Part A: Molecular and Biomolecular Spectroscopy* **2011**, *79* (5), 1034-1041.
48. Al-Marhaby, F.; Seoudi, R., Preparation and characterization of silver nanoparticles and their use in catalytic reduction of 4-Nitrophenol. *World Journal of Nano Science and Engineering* **2016**, *6* (01), 29.
49. Park, H. W.; Alam, S. M.; Lee, S. H.; Karim, M. M.; Wabaidur, S. M.; Kang, M.; Choi, J. H., Optical ascorbic acid sensor based on the fluorescence quenching of silver nanoparticles. *Luminescence* **2009**, *24* (6), 367-371.
50. Oldenburg, S. J., Silver nanoparticles: properties and applications. *Sigma-Aldrich Co.*, nd **2014**.
51. KK, S. R.; Rahman, P., Rhamnolipid biosurfactants-past, present, and future scenario of global market. *Frontiers in microbiology* **2014**, *5*, 454-454.
52. Kumar, C. G.; Mamidyala, S. K.; Das, B.; Sridhar, B.; Devi, G. S.; Karuna, M. S., Synthesis of biosurfactant-based silver nanoparticles with purified rhamnolipids isolated from *Pseudomonas aeruginosa* BS-161R. *J Microbiol Biotechnol* **2010**, *20*, 1061-1068.
53. Piste, P., Cysteine—master antioxidant. *Inter J Pharm Chem Biol Sci* **2013**, *3*, 143-149.
54. Hirayama, K.; Akashi, S.; Furuya, M.; Fukuhara, K.-i., Rapid confirmation and revision of the primary structure of bovine serum albumin by ESIMS and Frit-FAB LC/MS. *Biochemical and biophysical research communications* **1990**, *173* (2), 639-646.
55. Da, M., Bovine serum albumin.
56. Harmony, P., Harmonisation of reference intervals. 2013.
57. Connors, K. A., *Binding constants: the measurement of molecular complex stability*. Wiley-Interscience: 1987.